

Portland State University

PDXScholar

Dissertations and Theses

Dissertations and Theses

1987

Hyperbolic soil parameters for granular soils derived from pressuremeter tests for finite element programs

Dieter Neumann
Portland State University

Follow this and additional works at: https://pdxscholar.library.pdx.edu/open_access_etds



Part of the [Civil Engineering Commons](#)

Let us know how access to this document benefits you.

Recommended Citation

Neumann, Dieter, "Hyperbolic soil parameters for granular soils derived from pressuremeter tests for finite element programs" (1987). *Dissertations and Theses*. Paper 3718.

<https://doi.org/10.15760/etd.5602>

This Thesis is brought to you for free and open access. It has been accepted for inclusion in Dissertations and Theses by an authorized administrator of PDXScholar. Please contact us if we can make this document more accessible: pdxscholar@pdx.edu.

AN ABSTRACT OF THE THESIS OF Dieter Neumann for the Master of Arts in Civil Engineering presented on December 9, 1987.

Title: Hyperbolic Soil Parameters for Granular Soils
Derived from Pressuremeter Tests for Finite Element
Programs.

APPROVED BY MEMBERS OF THE THESIS COMMITTEE:

[REDACTED]

Trevor D. Smith, Chairman

[REDACTED]

Wendelin H. Mueller

[REDACTED]

Franz W. Rad

[REDACTED]

Michael J. Cummings

In the discipline of geotechnical Engineering the majority of finite element program users is familiar with the hyperbolic soil model. The input parameters are commonly obtained from a series of triaxial tests. For cohesionless soils however, todays sampling techniques fail

to provide undisturbed soil specimen. Furthermore, routine triaxial tests can not be carried out on soils with grains exceeding 10 - 15 mm in size.

In situ tests, such as the pressuremeter test, avoid many of the shortcomings inherent in the conventional soil investigation methods and are very cost effective.

The initial developments towards a link between high quality pressuremeter tests and the hyperbolic finite element input are presented. Theoretical and empirical approaches are used to determine the entire set of parameters from pressuremeter tests. Triaxial and pressuremeter tests are performed on the same soil. The proposed method is evaluated using a finite element program for axisymmetric solids modelling pressuremeter tests as well as a model foundation. The computer solutions are compared to the response of a physical model foundation under load application.

Further evaluation of the proposed method is accomplished using pressuremeter tests performed under field conditions in a severely cracked earth retaining structure. It has been shown that finite element modelling using pressuremeter data resulted in similar distress features as those observed at the real structure.

HYPERBOLIC SOIL PARAMETERS FOR GRANULAR SOILS
DERIVED FROM PRESSUREMETER TESTS
FOR FINITE ELEMENT PROGRAMS

by

Dieter Neumann

A thesis submitted in partial fulfillment of the
requirements for the degree of

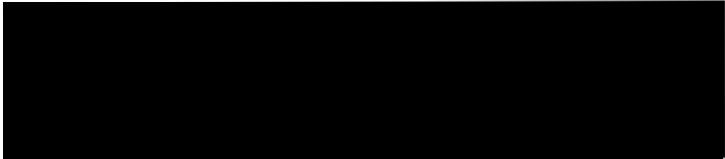
MASTER OF ARTS
in
CIVIL ENGINEERING

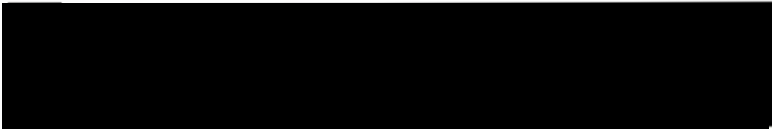
Portland State University

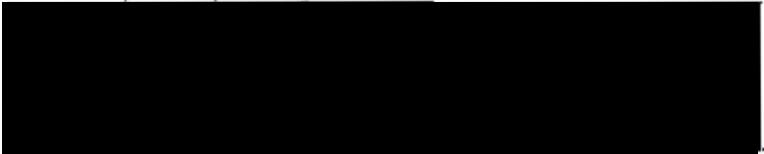
1987

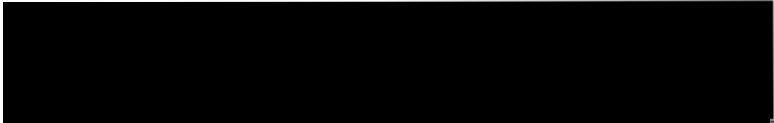
TO THE OFFICE OF GRADUATE STUDIES AND RESEARCH:

The members of the committee approve the thesis of
Dieter Neumann presented December 9, 1987.


Dr. Trevor D. Smith, Chairman


Dr. Wendelyn H. Mueller


Dr. Franz N. Rad


Dr. Michael J. Cummings

APPROVED: 


Dr. Franz N. Rad, Head, Department of Civil Engineering


Bernard Ross, Dean of Graduate Studies

DEDICATION

To:

Danuta, my wife and friend for all her support
and understanding,

and,

to those who fight for the preservation of the
beautiful nature of Australia, the Americas and
the world.

ACKNOWLEDGEMENTS

Gratefully acknowledged is the constructive and profound guidance by Prof. Dr. Trevor D. Smith in the progress of this study, whose professional efficiency and human composure make him an excellent teacher.

Of special importance were the many, most enjoyable, hours of formal and informal instruction and discussion of the pressuremeter as well as the applications of computerized solution techniques in geotechnical engineering.

Financially, this study was supported by a scholarship of the German Fulbright Commission, Bonn, West-Germany and by an award # 90-050-5801 8TS of the Office of Grants and Contracts at PSU.

The donation of the Willamette River sand by the Ross Island Sand & Gravel Company is much appreciated.

Finally, special thanks are extended to Anne Hotan of the PSU Computing Services, for her friendly and safe navigation through the jungle of peculiarities related to the CMS on the PSU mainframe computer.

TABLE OF CONTENTS

	PAGE
DEDICATION	iii
ACKNOWLEDGEMENTS	iv
TABLE OF CONTENTS	v
LIST OF TABLES	viii
LIST OF FIGURES	ix
CHAPTER	
I INTRODUCTION	1
Problem Description	1
Research Objective	2
II THEORETICAL BACKGROUND	4
Triaxial Test - Theory	4
Pressuremeter Test - Theory	6
Elastic Range	
Plastic Range	
III HYPERBOLIC SOIL MODELLING	17
Stress-Strain Relationships	17
Stress-Strain Parameters from Pressuremeter Tests	
Volume Change Relationships	32
Volume Change Parameters from Pressuremeter Tests	

CHAPTER		PAGE
	Conventional Parameters	40
	Conventional Parameters from Pressuremeter Tests	
IV	SOIL TESTING PROGRAM	45
	Selected Soil	45
	Triaxial Tests	45
	Sample Preparation Test Results	
	Pressuremeter Tests	55
	Placement Procedure Test Results	
V	FINITE ELEMENT STUDIES	61
	Introduction	61
	Finite Element Program AXISYM	62
	Volume Changes	
	Finite Element Analysis - Pressuremeter test	66
	Finite Element Analysis - Foundation	70
VI	MODEL FOUNDATION STUDY	76
	Model Foundation and Load Application	76
	Foundation Testing Procedure and Results	77

CHAPTER	PAGE
VII CASE HISTORY	80
Sand 'H' Debris Basin	80
VIII DISCUSSION OF THE RESULTS	83
Conclusions and Recommendations	84
LIST OF REFERENCES	87
LIST OF NOTATIONS	92
APPENDIX	95
Calculations for Hyperbolic Parameters, Triaxial Tests	96
Calculations for Hyperbolic Parameters, Pressuremeter Tests	99

LIST OF TABLES

TABLE		PAGE
I	Correction Factor α	27
II	Parameters for Sand - Handcalculated	53
III	Parameters for Sand - SP-5 Solutions	54
IV	Parameters for Sand from Pressuremeter Tests	60
V	Parameters used for Pressuremeter Analysis	68
VI	Parameters used for Foundation Analysis	72
VII	PMT Results from Sand 'H' Debris Basin	81
VIII	Hyperbolic Parameters Standard vs. PMT	82

LIST OF FIGURES

FIGURE	PAGE
1. Soil Sample in Triaxial Compression	6
2. Mohr Circles for Triaxial Test	6
3. PMT and the Surrounding Soil	9
4. Typical Pressuremeter Curve	10
5. Mohr Circles for PMT	14
6. Real Stress-Strain Hyperbola	18
7. Transformed Stress-Strain Hyperbola	18
8. Mohr-Coulomb Failure Envelope	20
9. Failure Ratio	20
10. Variation of E_i with Confining Pressure	22
11. Variation of Tangent Moduli	22
12. Variation of E_{ur} with Confining Pressure	25
13. Soil Moduli from Triaxial and Pressuremeter Tests with Increasing Confining Pressure	26
14. Variation of K_b with Confining Pressure	34
15. Bulk Modulus Exponent m as a Function of Relative Density	36
16. Bulk Modulus Number K_b as a Function of Relative Density	38

FIGURE

PAGE

17. Density Components of Strength ϕ'	42
18. Grain Size Distribution Curve for Willamette River Sand	46
19. Stress-Strain and Volume Change Curves for Willamette River Sand , $D_r = 50\%$	49
20. Stress-Strain and Volume Change Curves for Willamette River Sand , $D_r = 70\%$	50
21. Stress-Strain and Volume Change Curves for Willamette River Sand , $D_r = 95.6\%$	51
22. Pressuremeter Curve - Chamber Test, $D_r = 66\%$	57
23. Pressuremeter Curve - Drum Test I, $D_r = 67\%$	58
24. Pressuremeter Curve - Drum Test II, $D_r = 68\%$	59
25. Finite Element Mesh for Analysis of Pressuremeter Test	67
26. Variation of Pressuremeter Moduli with Increasing Depth	69
27. Finite Element Mesh for Analysis of Model Foundation	71
28. Load-Deflection Response for Model Foundation from AXISYM using Pressuremeter Parameters	73
29. Failure Generation During AXISYM Analysis	75
30. Load-Deflection Response as Measured for the Model Foundation	78

CHAPTER I

INTRODUCTION

The widespread use of digital computers and the development of powerful numerical schemes, such as the finite difference method or the finite element method, has increased the reliability of otherwise lengthy calculations and has provided the means to solve many problems for the first time. However, the precision of the computer solutions in mechanics is dependent upon the accurate determination of the material properties. This applies in particular to the discipline of geotechnical engineering, where still a great deal of empiricism is part of everyday practice.

PROBLEM DESCRIPTION

In the past two decades many formulations of nonlinear soil behavior have been published. The most successful being the hyperbolic soil model proposed by J.M. Duncan et al. (1980), and incorporated into numerous finite element programs solving a wide variety of geotechnical problems. Nevertheless, many of the shortcomings of classical solution procedures is still inherent.

The style and format of this thesis follows that used by the Journal of the Geotechnical Engineering Division, American Society of Civil Engineers.

The parameters describing the soil behavior are derived from conventional triaxial tests, where scale effects and disturbance of the samples may influence the reliability of the results significantly.

Today it is widely accepted that *in-situ* tests are more applicable for the accurate determination of soil parameters. This applies especially to granular soils where it is generally difficult to obtain undisturbed samples for conventional laboratory tests. Recompression of disturbed samples does not necessarily model the *in-situ* conditions because the *in-situ* density is difficult to measure.

Among all available devices testing the soil in place, the pressuremeter seems to be most superior since it reveals information about the soil prior to, and at failure. The fundamental idea of the pressuremeter is very well expressed if an "inside-out triaxial test" is considered. In addition to high quality design parameters, disturbed samples are obtained allowing visual examination and identification tests such as water content, Atterberg limits, or grain size distribution of the encountered soil.

RESEARCH OBJECTIVE

It is relevant to note that so far only very few attempts have been made to establish a link between the high quality soil information obtained from a pressuremeter test and the sophisticated soil model input for finite element

programs used frequently by engineers.

This thesis reports the initial developments towards a link between pressuremeter test results and finite element input. Theoretical considerations are employed in conjunction with pressuremeter tests, under laboratory conditions, to derive the soil parameters used in the hyperbolic soil model as input for the AXISYM (D.M. Holloway 1976) finite element program.

A finite element analysis of a simple foundation problem is performed where the parameters describing the soil behavior are based on pressuremeter testing. The predicted deflections are compared to the response of an instrumented physical model foundation tested on Willamette River sand. Reasonable agreement is found between the computer predicted and measured settlements. Finally, the derived equations are then applied to pressuremeter tests performed under field conditions, where good agreement with standard parameters is found.

CHAPTER II

THEORETICAL BACKGROUND

The hyperbolic, stress-dependent soil model proposed by J.M. Duncan et al. utilizes a total of nine parameters to describe the stress-strain characteristics of the soil. Three parameters, K , K_{UR} , and n , characterize the soil modulus in its elastic-plastic behavior limited by a failure ratio, R_f . Additionally, two terms, K_b and m , express the volume change characteristics of the soil medium, while three further, more conventional parameters, namely c , ϕ , and $\Delta\phi$, represent the shear and friction failure characteristics of the soil. A detailed description of the entire set of parameters is presented in Chapter III.

According to the recommended procedures, all of the above parameters are derived from triaxial compression tests. In order to prepare the theoretical background for the development of the above parameters derived from pressuremeter tests, a theoretical study of both soil investigation methods is presented.

TRIAXIAL TEST - THEORY

The triaxial compression test is a widely used laboratory test to determine shear strength and friction

parameters for soils and is certainly the most versatile laboratory test available. Volume changes and pore water pressure measurements are possible under a variety of stress states shown in detail by the classic work of A.W. Bishop and D.J. Henkel (1962).

It is of special significance to note that, contrary to what the test name might imply, it is not possible to induce any arbitrary stress condition to the triaxial sample. This would be the case in a true triaxial test, as proposed P.V. Lade (1979) or J.A. Pierce (1971), but no apparatus has yet been developed which is unquestionable.

A specimen in a conventional triaxial compression test is schematically displayed in Fig. 1. σ_2 and σ_3 are held equal and constant, usually by pneumatical means, while σ_1 is continuously increased to failure. Hence measured external principal stresses are applied to the sample. As the stress rises, readings of the applied axial load and the sample deformation are taken until the specimen fails by shearing on internal planes. The shear strength of the soil is determined from the applied axial load at failure. The maximum soil shear strength is given by the Mohr-Coulomb equation:

$$\tau_{\max} = c' + (\sigma - u) \cdot \tan \phi' \quad (2-1)$$

where c' is the cohesion intercept, σ is the total pressure normal to the plane in question, u is the pore pressure and ϕ' is the effective angle of internal friction (Fig. 2).

Specimen in Triaxial Compression

$$\sigma_2 = \sigma_3$$

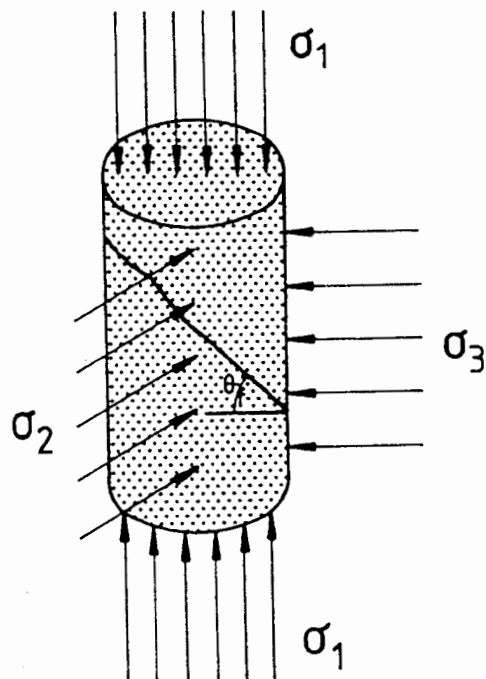


Figure 1. Soil Sample in Triaxial Compression.

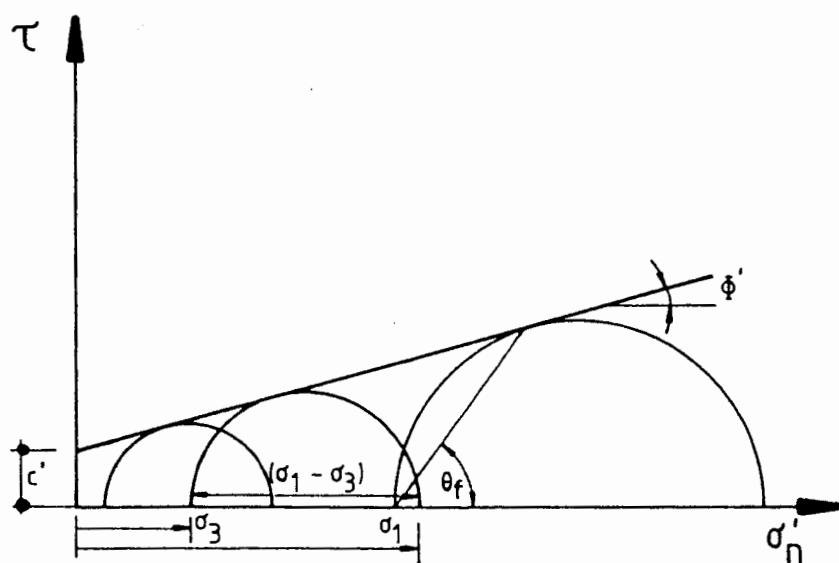


Figure 2. Mohr Circles for Triaxial Test.

The failure planes (Fig. 1) are inclined at an angle of

$$\theta_f = 45^\circ + \phi/2 \quad (2-2)$$

to the maximum principal plane, as can be seen from a typical plot of Mohr circles for a triaxial test (Fig. 2).

Conventional cohesion and friction parameters are determined from a series of tests at varying confining pressures.

PRESSUREMETER TEST - THEORY

The pressuremeter test is an *in-situ* soil test which was in principle presented by F. Kögler (1933), while further development was accomplished by L. Ménard (1957). Today, with nearly thirty years of sound theoretical and empirical development in France, the U.K., and Australia, where it has already found its place in routine soil investigations, the pressuremeter test is gradually emerging into geotechnical engineering practice of the U.S..

The pressuremeter is an inflatable probe which can be lowered down into a prebored or selfdrilled borehole. The test itself is carried out by applying internal principal stresses to the cavity by inflating the probe by either pneumatical or hydraulic means, or a combination of both. During expansion of the membrane, measurements of volume change and pressure are taken until the cavity has doubled

its initial volume.

Examination of the basic stress conditions in the soil mass surrounding the probe, given in Fig. 3, reveals the axisymmetric nature of the stress field as opposed to the cartesian coordinate system conventionally applied to the triaxial test. Not only are different coordinates used, but also an entirely different set of parameters is procured, providing the basis for settlement and bearing capacity calculations.

For the case of a prebored test, stress relief takes place upon borehole drilling and the first part of a typical pressure-volume change curve for a pressuremeter test, as given in Fig. 4, represents the reloading of the soil to its initial stress condition. Further stress increase exposes a linear, elastic response of the soil, from which the pressuremeter modulus, E usually is calculated by the elasticity relationship given by Eq. 2-3.

$$E = 2 \cdot (1 + \nu)G \quad (2-3)$$

where poisson's ratio is frequently assumed to be 0.33 and G is the shear modulus measured during the cavity expansion as defined by Eq. 2-4.

$$G = V_{AV} \cdot \frac{\Delta p}{\Delta V} \quad (2-4)$$

In this expression Δp is the change in radial pressure, ΔV is the change in cavity volume and V_{AV} is the average cavity

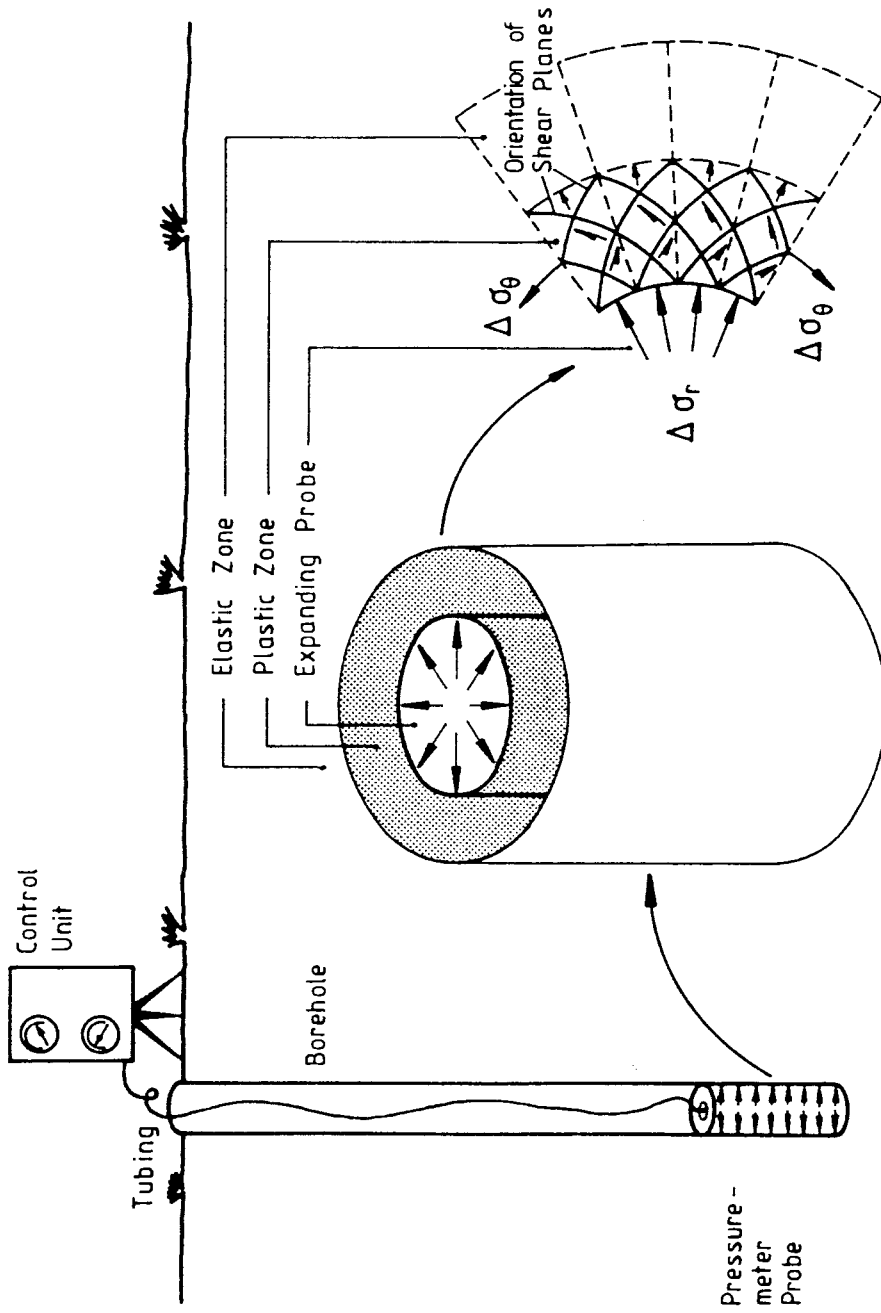


Figure 3. PMT and the Surrounding Soil.

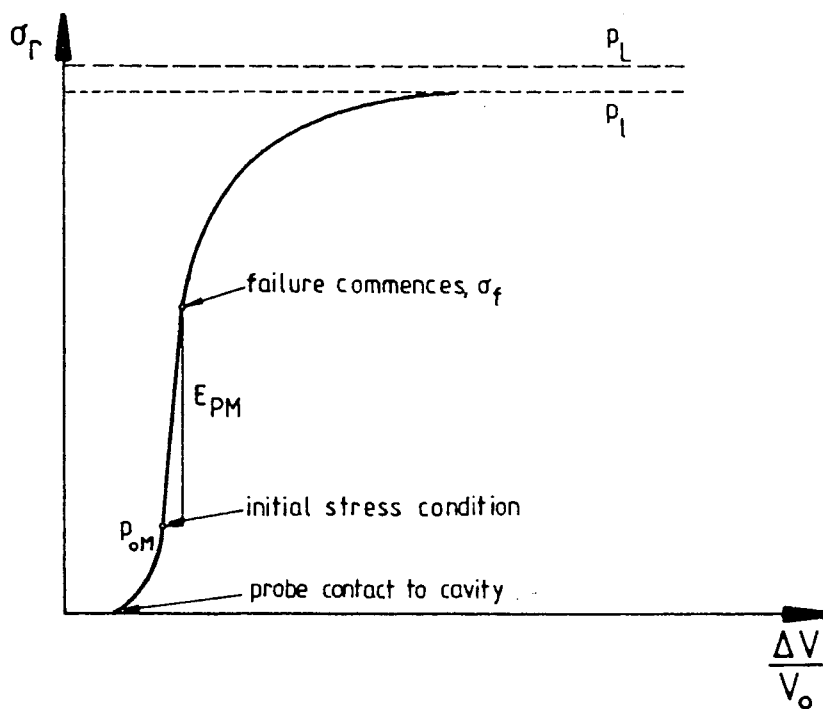


Figure 4. Typical Pressuremeter Curve.

volume.

Finally, upon continued cavity expansion the soil yields and the plastic range of the soil is reached. While the soil particles close to the probe have failed already, more outer particles are just becoming distorted and move from elastic through plastic response as further expansion takes place. For this reason, two different sets of rheological equations need to be considered to represent the pressuremeter test in its full range.

In most current pressuremeter theories the following assumptions are made:

1. Distortions occur only in the horizontal plane, that is plane strain. J.P. Hartman (1974) showed, using C.J. Tranter's (1946) closed form solution, that only small differences exist between the expansion of a cavity with finite and infinite length. J.-L. Briaud, L.M. Tucker and C.A. Makarim (1985) recommend the use of probes with a minimum L/D ratio of 6.5.
2. End effects at the membrane ends are negligible, allowing the assumption of an ideally cylindrical cavity.
3. The soil is assumed to be an isotropic, elastic material.
4. Poisson's ratio is frequently assumed as $\nu = 0.33$ and a Menard modulus $E_M = 2.66 \cdot G$ is obtained.

Pressuremeter Test - Elastic Range

In the pressuremeter test, only the soil in the immediate vicinity of the probe is stressed through its full range of stresses, radial strains decay with the square of the distance dramatically, F. Baguelin, J.-F. Jezequel and D.H. Shields (1978), as can be seen from Eq. 2-5.

$$\epsilon_r = - \frac{\epsilon_0 \cdot r_0^2}{r^2} \quad (2-5)$$

in which ϵ_r is the radial strain, ϵ_0 is the strain at the cavity wall, r_0 is the initial radius of the cavity and r is the radial distance to a point in the surrounding soil mass.

In axisymmetrical problems, any radial displacement automatically induces strain in the circumferential direction. Radial and circumferential stresses are principal stresses by reasons of symmetry. The radial stress, σ_r , is increasing as the probe expands against the borehole wall, while the circumferential stress, σ_θ , is decreasing about an equal amount, F. Baguelin, J.-F. Jezequel and D.H. Shields (1978), (Eq. 2-6).

$$\Delta\sigma_r = -\Delta\sigma_\theta = 2G \cdot \frac{\epsilon_0 \cdot r_0^2}{r^2} \quad (2-6)$$

So that the radial stress at a point becomes

$$\sigma_r = p_0 + 2G \cdot \frac{\epsilon_0 \cdot r_0^2}{r^2} \quad \dots \dots \dots (2-7)$$

where p_0 is the initial horizontal soil pressure. The circumferential stress then becomes

$$\sigma_\theta = p_0 - 2G \cdot \frac{\epsilon_0 \cdot r_0^2}{r^2} \quad \dots \dots \dots (2-8)$$

Mohr circles for the stress changes in a particular element, shown in Fig. 5, demonstrate that the average all around stress, that is σ_{oct} , is unchanged and hence,

$$\Delta\sigma_{oct} = \frac{\Delta\sigma_r + \Delta\sigma_\theta + \Delta\sigma_z}{3} \quad \dots \dots \dots (2-9)$$

where σ_z is the vertical stress. Nevertheless, the principal stress difference, $(\sigma_1 - \sigma_3)$, increases.

Failure planes are inclined $45^\circ + \phi/2$ to the principal stress directions where the maximum shear stress occurs as given by Eq. 2-10.

$$\tau_{max} = \frac{\sigma_r - \sigma_\theta}{2} \quad \dots \dots \dots (2-10)$$

However, it must be clearly recognized that elastic soil is only realistic in the range of small strains, say up to 5% and hence, to represent the pressuremeter expansion in

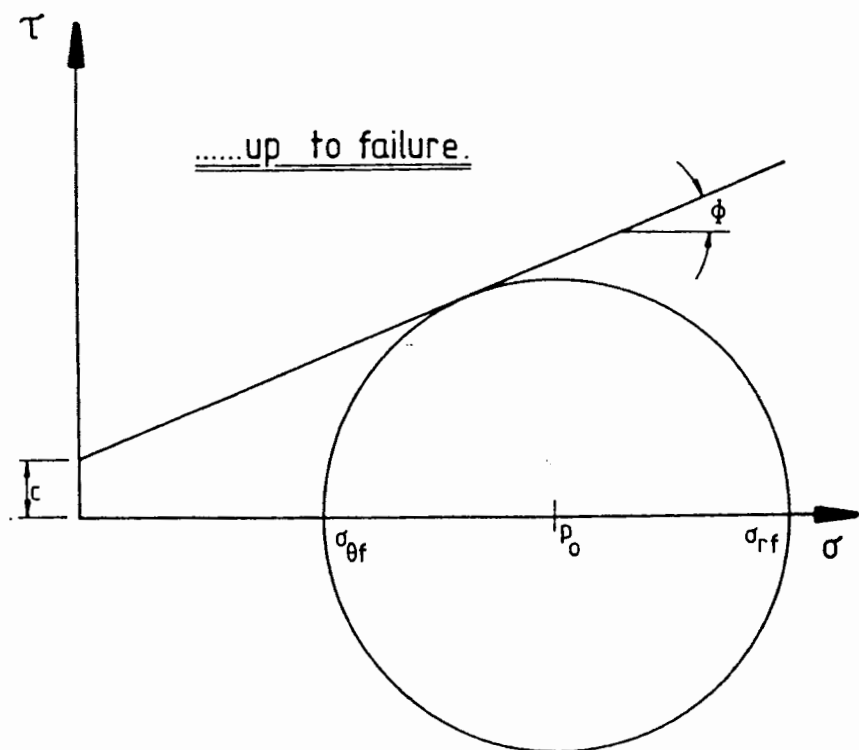
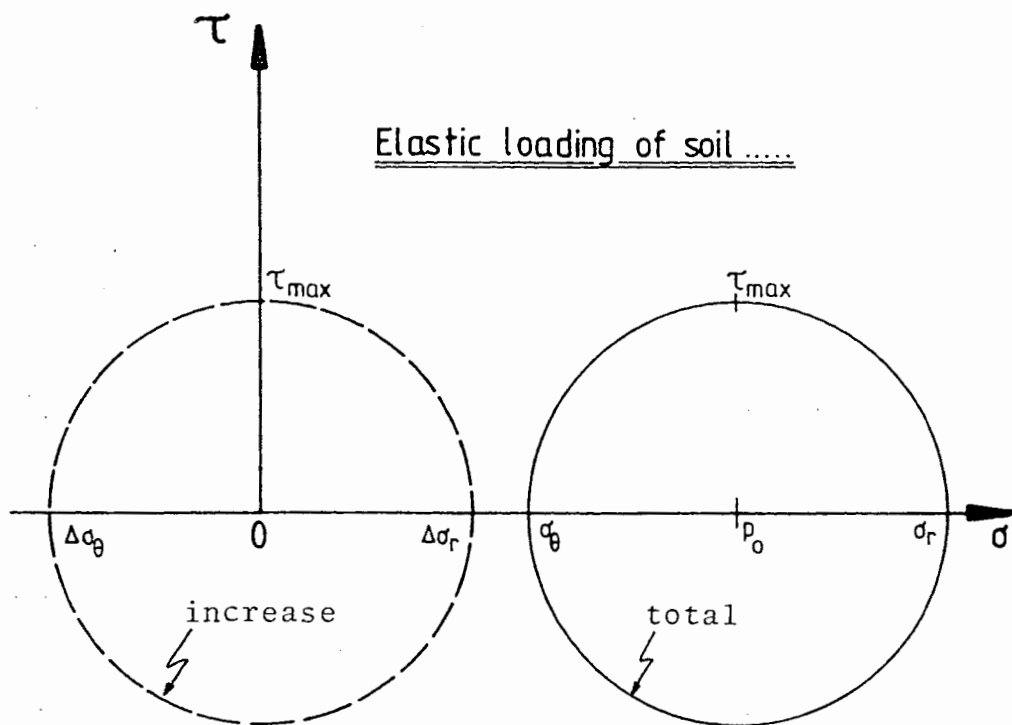


Figure 5. Mohr Circles for PMT.

its full range, additional factors are to be considered.

Pressuremeter Test - Plastic Range

Considering a soil with cohesion and friction, F. Baguelin J.-F. Jezequel and D.H. Shields (1978) showed that the well understood Mohr-Coulomb failure criterion can be written for the pressuremeter test as:

$$\sigma_\theta + c \cdot \cot \phi = K_a \cdot (\sigma_r + c \cos \phi) \quad (2-11)$$

where

$$K_a = \tan^2 \cdot (\pi/4 - \phi/2) \quad (2-12)$$

and is the active earth pressure coefficient. The theoretical limit pressure at infinite expansion is given by

$$p_L = (p_o + c \cot \phi) \cdot (1 + \sin \phi) \cdot \left[\frac{1}{2 \cdot \alpha_f} \right]^{\frac{1-K_a}{2}} - c \cot \phi \quad . . . (2-13)$$

as opposed to the practical limit pressure, p_1 , which is somewhat lower than p_L , since p_1 is, by definition, reached when the initial cavity volume has been doubled and is expressed by

$$p_1 = (\sigma_f + c \cot \phi) \cdot \left[\frac{1}{4 \cdot \alpha_f} \right]^{\frac{1-K_a}{2}} - c \cot \phi \quad . . . (2-14)$$

The *almansi* strain, α_f in Eqs. 2-13 and 2-14 becomes,

$$\alpha_f = \frac{\sigma_f - P_0}{G} \quad (2-15)$$

and the stress at the onset of failure is expressed by,

$$\sigma_f = P_0 + (P_0 + c \cdot \cot \phi) \cdot \sin \phi \quad (2-16)$$

$$\sigma_f = P_0 \cdot (1 + \sin \phi) + c \cdot \cos \phi \quad (2-17)$$

Most of the above equations simplify considerably for a purely frictional material because of the absence of cohesion.

CHAPTER III

HYPERBOLIC SOIL MODELLING

STRESS-STRAIN RELATIONSHIPS

R.L. Kondner (1963) showed that a two-constant hyperbola, represented by Eq. 3-1, was most suitable to fit to a high degree of precision the stress-strain curves of many soils (Fig. 6). Noteworthy is that an identical expression was proposed 110 years earlier by H. Cox (1850) in his hyperbolic law of elasticity for metals. Both expressions are of the form :

$$(\sigma_1 - \sigma_3) = \frac{\epsilon_a}{a + b\epsilon_a} \quad \dots \dots \dots (3-1)$$

Where σ_1 is the major principal stress, σ_3 is the minor principal stress, and ϵ_a is the axial strain, while a and b are constants. Transformation of Eq.3-1 into its linear form yields Eq. 3-2, presented in Fig. 7.

$$\frac{\epsilon_a}{(\sigma_1 - \sigma_3)} = a + b\epsilon_a \quad \dots \dots \dots (3-2)$$

Inspection of Fig. 6 and 7 reveals that a and b are meaningful physical parameters. R.L. Kondner and S.S. Zelasko (1963) showed that ' a ' represents the reciprocal of the initial tangent modulus, E_i , while b is the

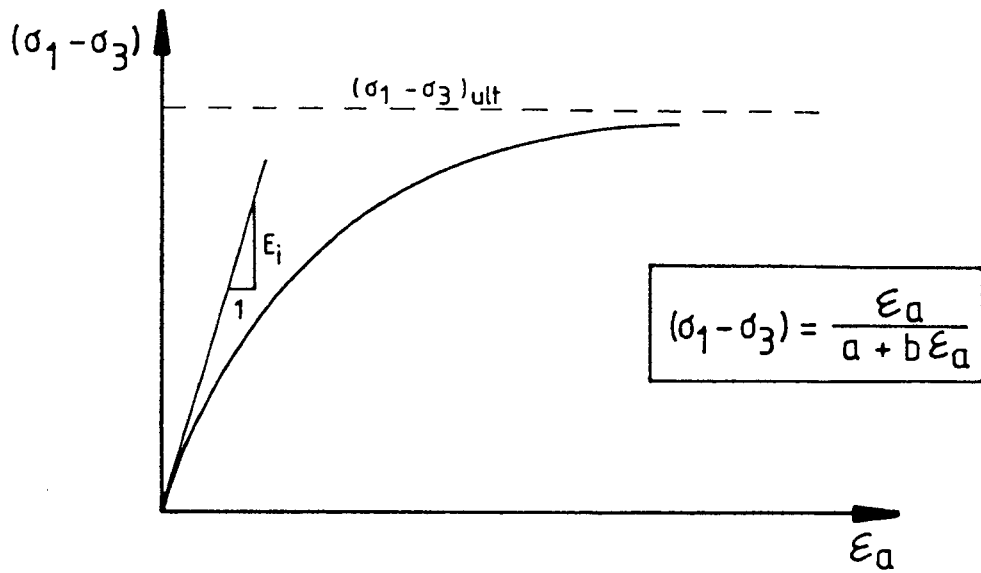


Figure 6. Real Stress-Strain Hyperbola.

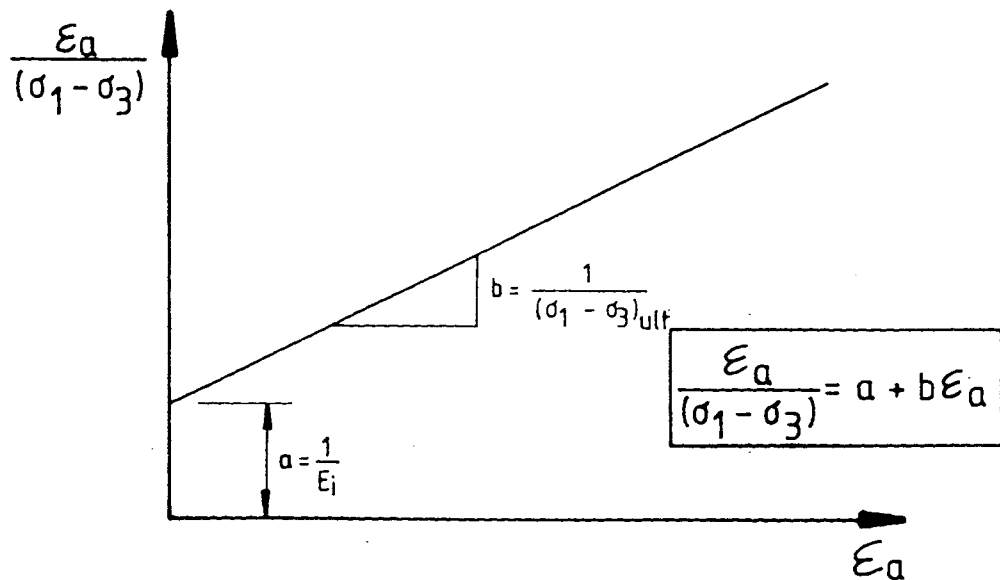


Figure 7. Transformed Stress-Strain Hyperbola.

reciprocal of the ultimate normal stress difference, known as the deviator stress $(\sigma_1 - \sigma_3)_{ult}$ and serving as the asymptote of the hyperbola.

The actual values of a and b are coventionally derived by plotting triaxial test data on the transformed plot, where the best fitting straight line corresponds to the best fitting hyperbola on the stress-strain plot.

Then $(\sigma_1 - \sigma_3)_{ult}$ is found to be greater than the stress difference expressed by the Mohr-Coulomb failure envelope (Fig. 8) and it can be shown, given by Eq. 3-3,

$$(\sigma_1 - \sigma_3)_f = \frac{2 c \cos \phi + 2 \sigma_3 \sin \phi}{1 - \sin \phi} \quad . . . (3-3)$$

in which c is the cohesion and ϕ is the angle of internal friction. Assuming the above criterion is still valid at failure, this difference is accounted for by introducing a parameter called the failure ratio, R_f .

$$R_f = \frac{(\sigma_1 - \sigma_3)_f}{(\sigma_1 - \sigma_3)_{ult}} \quad (3-4)$$

Graphically the effect of this multiplier on the modelled stress-strain curve is displayed in Fig. 9.

N. Janbu (1963) recommended the use of an initial tangent modulus, as defined by Eq. 3-5, as an appropriate measure of the compressibility of soils ranging from solid rock to plastic clays.

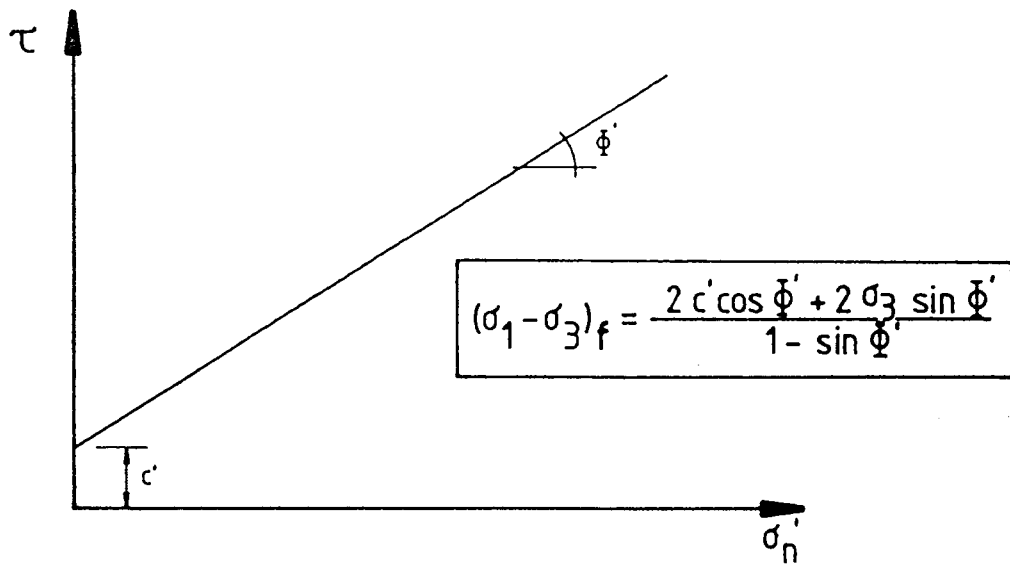


Figure 8. Mohr-Coulomb Failure Envelope.

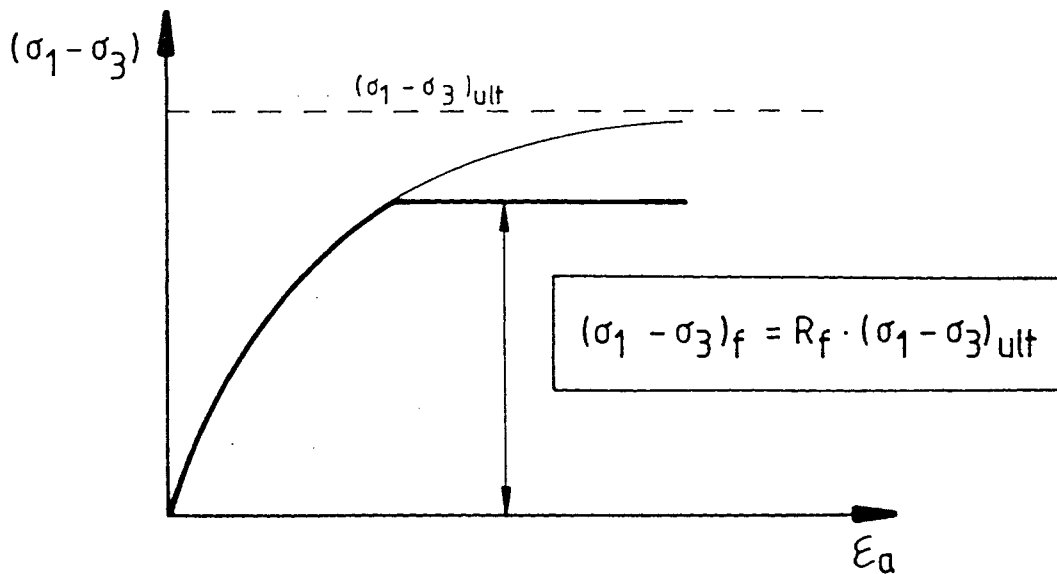


Figure 9. Failure Ratio.

$$E_i = K \cdot P_a \cdot \left[\frac{\sigma_3}{P_a} \right]^n \quad \dots \dots \dots (3-5)$$

Where P_a is the atmospheric pressure, K and n are modulus number and modulus exponent, respectively, relating E_i , the initial tangent modulus, to the confining pressure, σ_3 . Based on triaxial tests, the actual values of both K and n are determined by plotting the results for E_i and σ_3 of a series of tests on a log-log scale, as in Fig. 10. From the best fitting straight line, K is found as the intercept on the vertical axis, while n is the slope of the line. Both parameters are dimensionless numbers.

While the initial tangent modulus defines the initial portion of the stress-strain curve, the remaining part is represented by a simple tangent modulus as given by Eq. 3-4, which is graphically displayed in Fig. 11.

$$E_t = \frac{\partial(\sigma_1 - \sigma_3)}{\partial \epsilon_a} \quad \dots \dots \dots (3-6)$$

J.M. Duncan and C.Y. Chang (1970) showed that the tangent modulus might also be expressed independently of stress and strain as:

$$E_t = (1 - R_f \cdot S)^2 \cdot E_i \quad \dots \dots \dots (3-7)$$

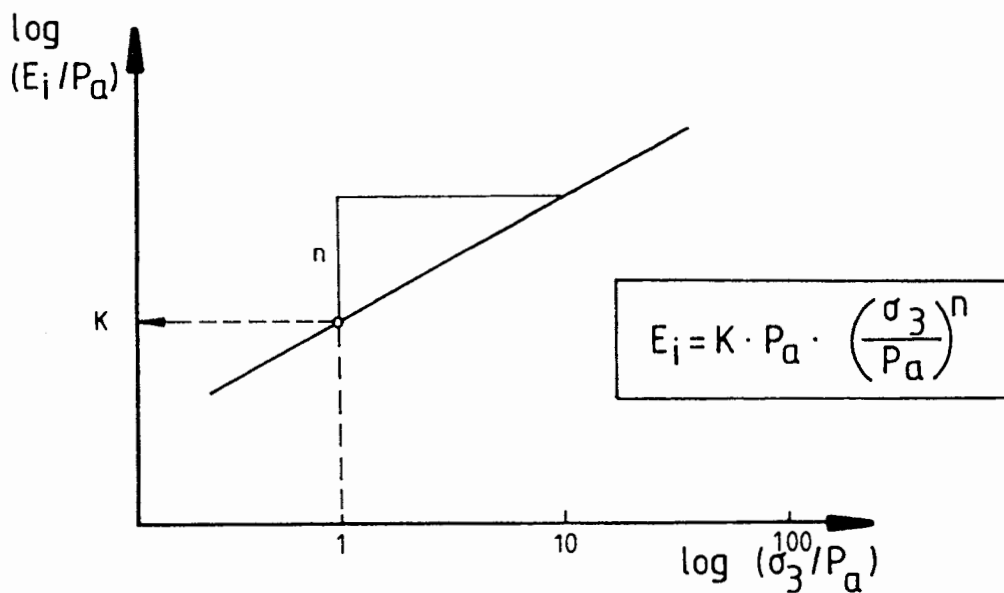


Figure 10. Variation of E_i with Confining Pressure.

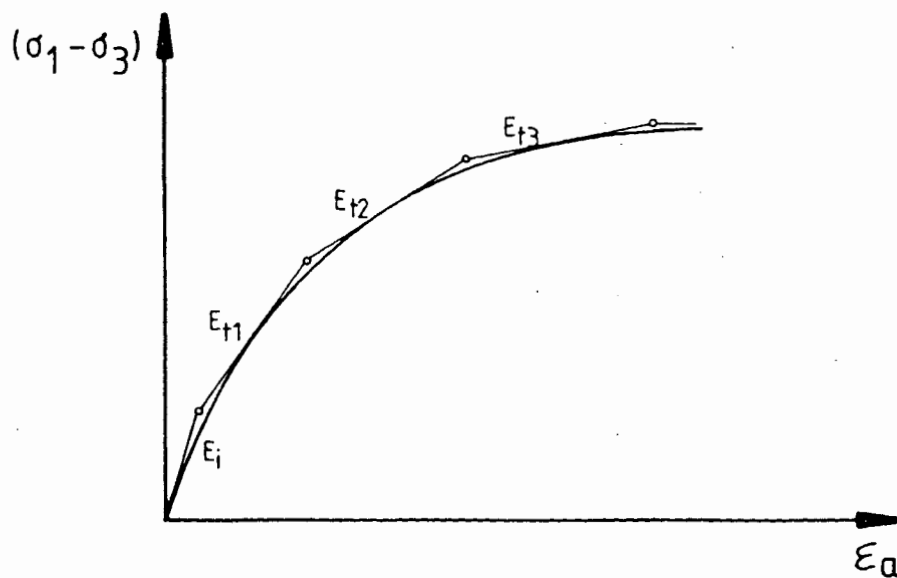


Figure 11. Variation of Tangent Moduli.

where S , the stress level, is expressed as:

$$S = \frac{(\sigma_1 - \sigma_3)}{(\sigma_1 - \sigma_3)_f} \quad (3-8)$$

Substituting the expressions for S , $(\sigma_1 - \sigma_3)_f$, and E_i as given by Eqs. 3-8, 3-3, and 3-5 into Eq. 3-7 yields the following expression for the tangent modulus at any stress state.

$$E_t = \left[1 - \frac{R_f \cdot (1 - \sin \phi) \cdot (\sigma_1 - \sigma_3)}{2 c \cos \phi + 2 \sigma_3 \sin \phi} \right]^2 \cdot K \cdot P_a \cdot \left[\frac{\sigma_3}{P_a} \right]^n \quad (3-9)$$

In the case of an element undergoing shear failure, i.e. the Mohr-Coulomb strength relationship as expressed in Eq. 3-3 is exceeded, the value of the tangent modulus is defaulted to a very small number, being equivalent to a very soft soil. The element has failed and for a slight increase in stresses large deflections are observed, not unlike "plastic" behavior.

The fact that the stress-strain relationship of the soil is modelled hyperbolically shows quite readily that soil is by no means behaving elastically. This implies that a soil element once deformed will not recover its initial shape if the applied load is removed. Furthermore, if the element is reloaded, possibly beyond the previous stress level, the unload-reload cycle is steeper than the initial

stress-strain response due to the first load application. This phenomenon is shown in Fig. 12.

The expression for the unload-reload modulus, E_{ur} is given by Eq. 3-10.

$$E_{ur} = K_{ur} \cdot P_a \cdot \left[\frac{\sigma_3}{P_a} \right]^n \quad \dots \dots \dots (3-10)$$

It should be noted that the modulus exponent is the same as the one used in Eq. 3-5. J.M.Duncan et al. (1980) state depending on the soil type, the actual value of K_{ur} might be in the range of 1.2 times the value for K , as in the case of a stiff soil, but could climb up to three times the value of K in the case of very soft soils.

Stress-Strain Parameters from PMT

It is clearly recognized that, especially for granular soils, the stress-strain response is highly dependent upon confining pressure, that is to say modulus values in an isotropic soil increase with depth, as shown in Fig. 13. A very similar observation was made by L.D. Johnson (1986), comparing pressuremeter moduli with first load moduli from undrained triaxial tests on Midway clay. Both were increasing linear with depth.

The evidence, however, is that the pressuremeter modulus cannot be compared directly with a compression modulus such as the Young's modulus, since the stress paths

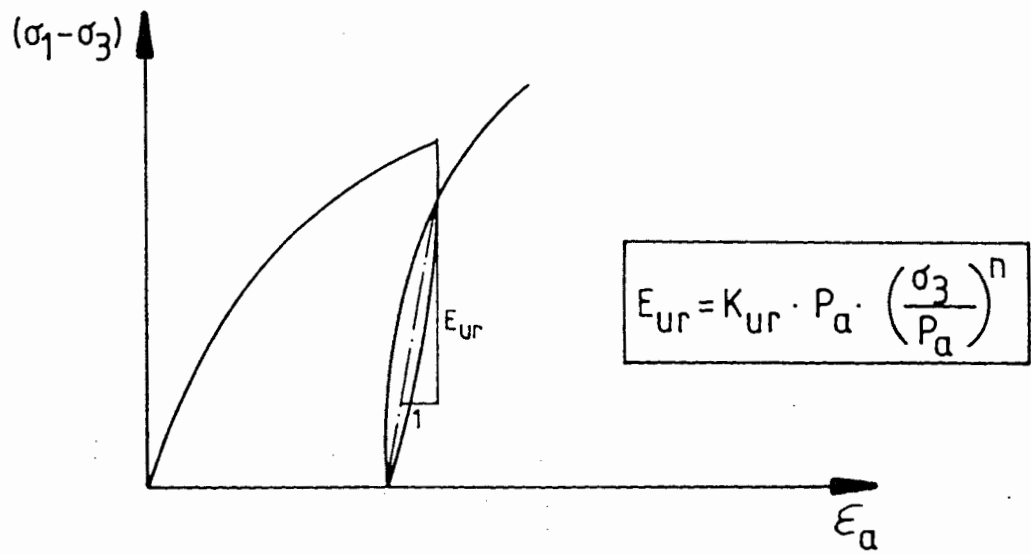


Figure 12. Variation of E_{ur} with Confining Pressure.

SOIL MODULI FROM TRIAXIAL AND PRESSUREMETER TESTS AT VARYING CONFINING PRESSURES

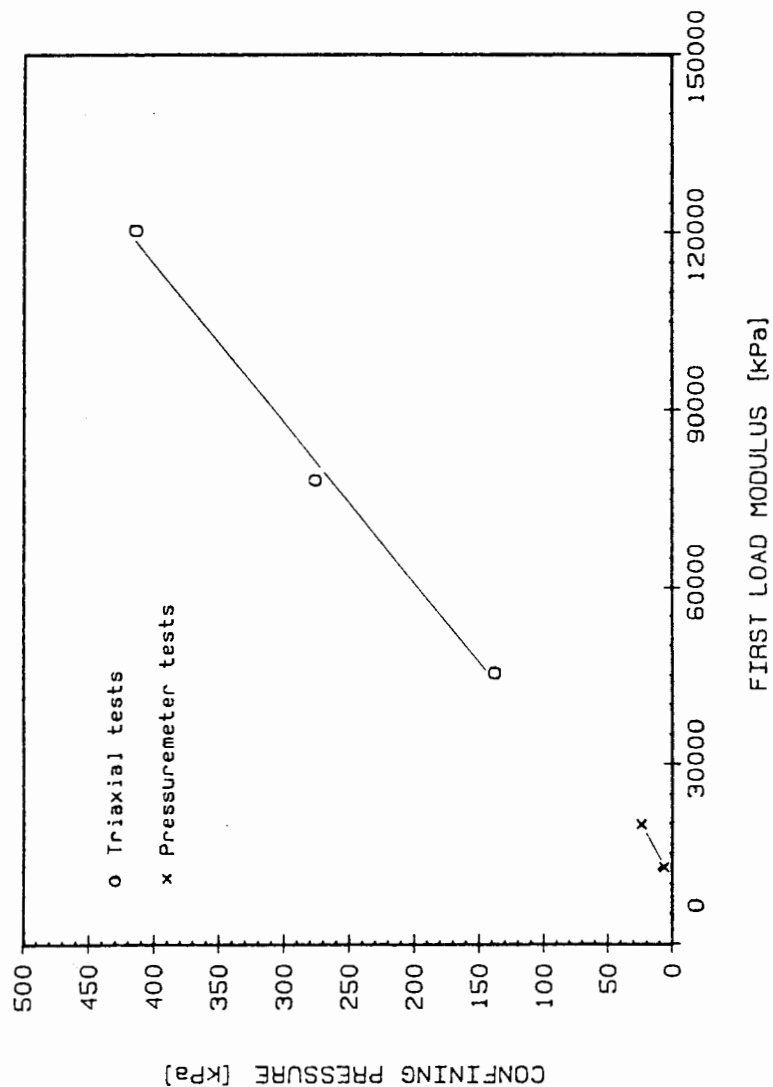


Figure 13. Soil Moduli from Triaxial and Pressuremeter Tests with Increasing Confining Pressure.

followed are different in pressuremeter and traditional compression tests. A comparison of Ménard moduli, E_M and soil moduli, E_S (obtained from traditional soil investigation methods) indicates that E_S might be anywhere from 2 to 10 times higher than E_M (F. Baguelin, J.F. Jezequel and D.H. Shields, 1978).

Investigating the pressuremeter modulus, E_M at very small strains, L. Ménard (1961) states that the so called modulus of "micro-deformation", E_m , is usually in the order of 3 times E_M (but for certain soils might be as high as 20 times E_M). Based on the ratio E_M/p_1 an empirical correction factor, α has been determined (Centre d'Etudes Ménard, 1975) to account for the above mentioned differences as given in Table I.

TABLE I
CORRECTION FACTOR α

Type of Soil	Silt		Sand		Sand and Gravel	
	E_M/p_1	α	E_M/p_1	α	E_M/p_1	α
Overconsolidated	>14	2/3	>12	1/2	>10	1/3
Normally consolidated	8-14	1/2	7-12	1/3	6-10	1/4
Weathered and Remoulded		1/2		1/3		1/4

The modified pressuremeter modulus, E_{PM} is then,

$$E_{PM} = E_M / \alpha \quad (3-11)$$

which is still a secant modulus rather than an initial tangent modulus as used in the hyperbolic soil model. If the corrected pressuremeter modulus is used, it seems intuitively appropriate to use a modified version of Eq. 3-5 as given by the following.

$$E_{PM} = K_{PM} \cdot P_a \cdot \left[\frac{\sigma_z'}{P_a} \right]^s \quad (3-12)$$

Where K_{PM} and s are modulus number and modulus exponent respectively, based on pressuremeter tests. E_{PM} is the first loading modulus as obtained from the pseudo-elastic portion of the pressuremeter curve. σ_z' is the effective overburden pressure and represents a conservative estimate of the confining pressure. The actual values of both K_{PM} and s are determined by plotting the results for E_{PM} and σ_z' for a series of tests at increasing depth on a log-log scale, analogous to the triaxial test procedure. From the best fitting straight line K_{PM} is then found as the intercept on the vertical axis, while s is the slope of the line. Both parameters are, again, dimensionless numbers.

The above expression describes the variation of the pressuremeter modulus with depth in terms of overburden

pressure. A very similar relationship is proposed for the unload-reload behavior. As in triaxial tests, an increase of the soil modulus is noticed if an unload-reload cycle is performed during a pressuremeter test. The variation is similar in both pressuremeter and triaxial tests, so Eq. 3-13 is proposed.

$$E_{Pur} = K_{Pur} \cdot P_a \cdot \left[\frac{\sigma_z'}{P_a} \right]^s \quad \dots \dots \dots (3-13)$$

The modulus exponent, s , remains unchanged from Eq. 3-12 and the modulus number, K_{Pur} , is obtained in a similar fashion as for the triaxial test.

In the hyperbolic soil model, the permitted range of stresses is limited by the failure ratio, R_f . This is for triaxial tests the ratio of the measured peak strength to the theoretical maximum strength using a hyperbolic function.

If the Mohr-Coulomb failure criterion, as given by Eq. 2-9, is assumed valid at failure, the radial stress, σ_r , becomes the radial stress at the onset of plastic behavior, σ_f . This is the point on the pressuremeter curve at which failure commences, initiated at the wall of the cavity. Further expansion of the cavity, up to 100 % volumetric strain, marks the end of the pressuremeter curve where the practical limit pressure, p_l (Eq. 2-14), is reached. The theoretical maximum resistance the soil could mobilize, at

infinite cavity expansion, is given by p_L (Eq. 2-13).

In direct analogy to the triaxial test, Eq. 3-14 gives the proposed relationship for a failure ratio based on pressuremeter tests.

$$R_{pf} = \frac{p_i}{p_L} \quad (3-14)$$

Considering an entirely frictional material, the expressions for p_i and p_L can be simplified and substitution of both expressions into Eq. 3-14 gives,

$$R_{pf} = \frac{\frac{\sigma_f \cdot (1/4\alpha_f)^2}{1-K_a}}{\frac{\sigma_f \cdot (1/2\alpha_f)^2}{1-K_a}} \quad (3-15)$$

In order to determine K_a , the angle of internal friction has to be known and might be computed either by backcalculation using p_i (as measured or by interpretation) or σ_f .

Substitution of Eq. 2-15 into the above expression yields

$$R_{pf} = \frac{\frac{\sigma_f \cdot [G/(2\sigma_f - 2p_0)]^2}{1-K_a}}{\frac{\sigma_f \cdot [G/(\sigma_f - p_0)]^2}{1-K_a}} \quad (3-16)$$

where the nominator might be taken as the practical limit

pressure, p_1 . For a series of tests, as recommended herein, the actual value of R_{pf} is determined as the average of the calculated values from each test.

VOLUME CHANGE RELATIONSHIPS

J.M. Duncan et al. (1980) showed that a bulk modulus as defined by Eq. 3-17 could express the volume change characteristics of a soil with good accuracy.

$$B = \frac{\Delta\sigma_1 + \Delta\sigma_2 + \Delta\sigma_3}{3 \cdot \epsilon_{v01}} \quad \dots \dots \dots (3-17)$$

Where ϵ_{v01} is the volumetric strain. For the conventional triaxial test, this expression reduces to

$$B = \frac{(\sigma_1 - \sigma_3)}{3 \cdot \epsilon_{v01}} \quad \dots \dots \dots (3-18)$$

because the deviator stress increases while the confining pressure is held constant and $\sigma_2 = \sigma_3$. Hence, B might be calculated using any point on the stress-strain curve and its corresponding point of the volume change curve.

Investigating the effect of varying confining pressure, σ_3 , on the bulk modulus, Duncan and his co-workers found B to be a function of the confining pressure, analogous to the initial tangent modulus.

$$B = K_b \cdot P_a \cdot \left[\frac{\sigma_3}{P_a} \right]^m \quad \dots \dots \dots (3-19)$$

In which K_b is the bulk modulus number and m is the bulk

modulus exponent. The procedure for the determination of bulk modulus number and exponent is similar as for the determination of K and n and can readily be seen in Fig. 14.

For the use of this soil model in finite element programs, (this is the prime reason for the development of such a soil model), the range of the bulk modulus has to be limited in order to avoid certain values of poisson's ratio. This can be visualized by substituting values of $\nu \rightarrow 0.5$ into Eq. 3-20, which is the equation for the bulk modulus assuming elastic behavior.

$$B = \frac{E}{3 \cdot (1-2\nu)} \quad (3-20)$$

A further, more detailed discussion on this aspect is presented in Chapter V.

Volume Change Parameters from PMT

Soil volume changes are not directly measured during a pressuremeter test because they occur externally, even indirect measurements by interpretation of pore water pressure changes during probe expansion, are not taken on a routine basis. Therefore, no clear cut solution for the representation of volume changes can be derived. However, since volume changes are of significance for granular soils, compared to clays, they can not be neglected. In fact, a wide range of volume changes from contraction (loose material) to expansion (dense material) has to be

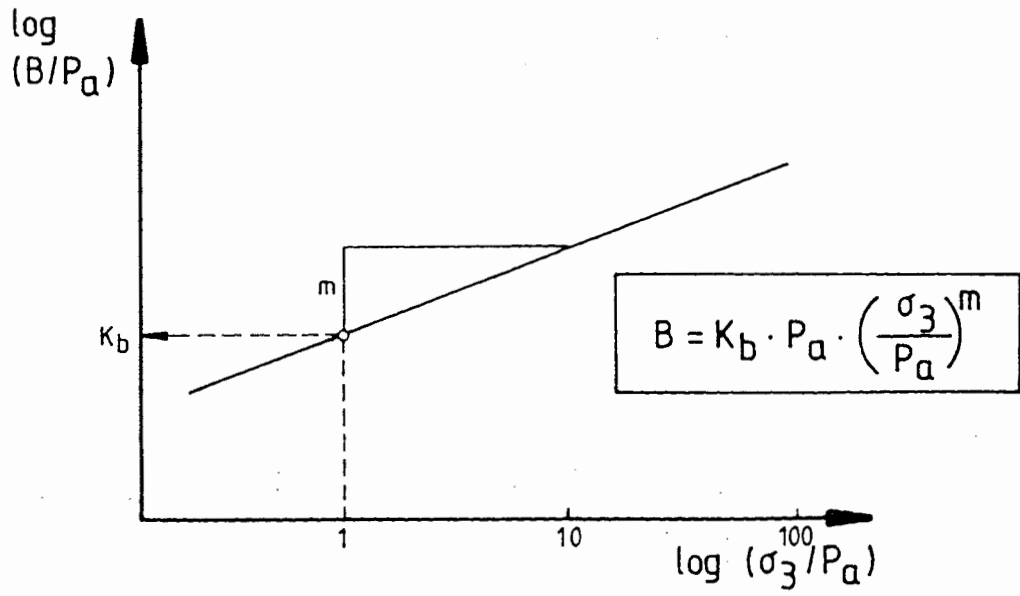


Figure 14. Variation of K_b with Confining Pressure.

considered. For a cohesionless soil, poisson's ratio might be expected in the range between 0.3 - 0.4.

The significance of volume changes has been the subject of many parametric studies by various researchers. J.P. Hartman's (1974) findings indicate that, for a linear elastic material as well as for a nonlinear material obeying the hyperbolic relationships, the calculated pressuremeter moduli are independent of poisson's ratio. Nevertheless, a significant effect on the limit pressure is found to be related to a change in ν .

Considering the foregoing, a way out of the dilemma might be the correlation of changes in volume to some other relevant soil property or parameter. All indications show that volume changes are highly dependent on the relative density of the soil, and to a lesser extent on grain size and shape. Based on available triaxial test data, correlations of relative density to the bulk modulus exponent and bulk modulus number have been investigated. The incorporated data was published by J.M. Duncan et al. (1980) and H. Schad (1979) and represents only excellent quality information, i.e. using the hyperbolic parameters the backcalculated stress-strain curves are in very good agreement to those measured.

A range of bulk modulus exponent values for granular soils, ranging from sandy gravels to silty sands, has been established and is graphically displayed in Fig. 15 (data

VARIATION OF m AS A FUNCTION OF DENSITY

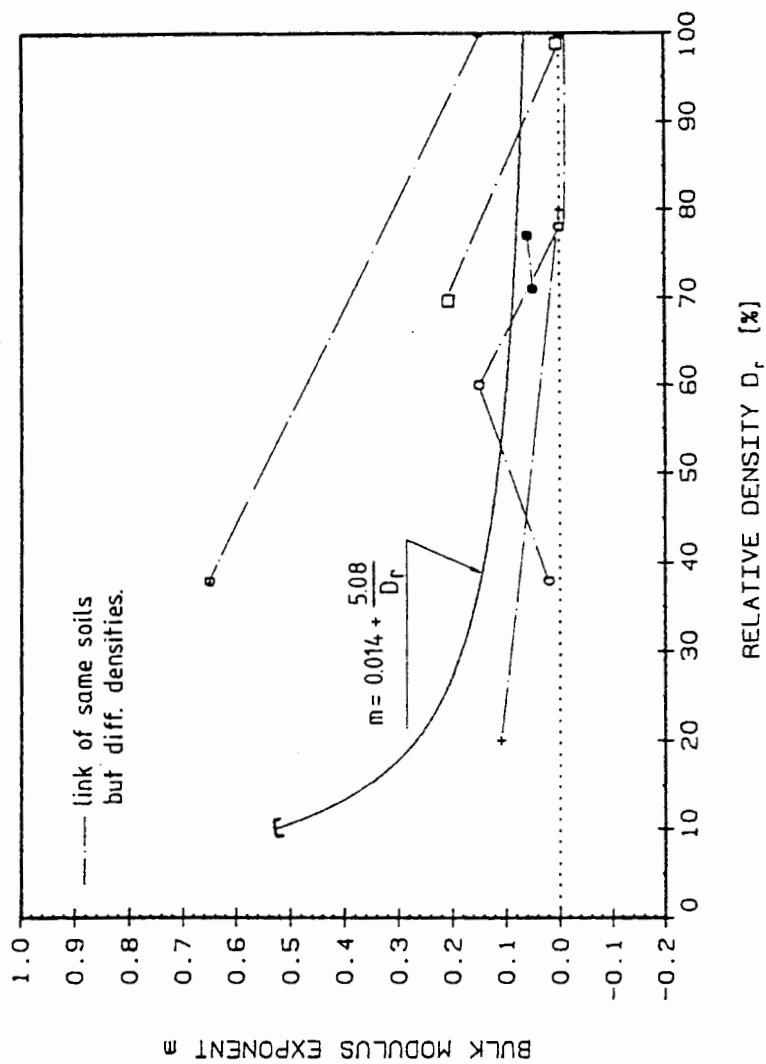


Figure 15. Bulk Modulus Exponent m as a Function of Relative Density.

points corresponding to identical soils are connected). In general, it can be stated that the bulk modulus exponent, m , is decreasing with increasing density. Moreover, in densities exceeding 70 % is practically zero. Hence the bulk modulus, B , shows a linear increase at higher densities independently of confining pressures. A multiple regression analysis of the accumulated data was performed and a correlation as given by Eq. 3-21 was obtained.

$$m = 0.014 + 5.08 \cdot 1/D_r \quad (3-21)$$

where D_r is used in %. Fig. 15 also displays the curve representing the above equation. It should be noted that only values of $D_r > 10$ % should be used.

M.G. Katona et al. (1981) recommended in the CANDE manual the use of a standard bulk modulus exponent of $m = 0.2$ for granular aggregates with densities ranging from 21.2 - 23.6 kN/m³. Katona's recommendation is based on an extensive collection of hyperbolic parameters given by J.M. Duncan et al. (1980). The given range of densities relates to a relative density of approximately 75 % to 100 %. A fairly good correlation to the typical value of $m = 0.2$ is recognized upon inspection of the graph.

A similar procedure was followed for the bulk modulus number, K_b , for which the data base and the regression curve is given in Fig. 16. Even though the scatter of the data points is larger than for the exponent, it was found that K_b

VARIATION OF K_b AS A FUNCTION OF DENSITY

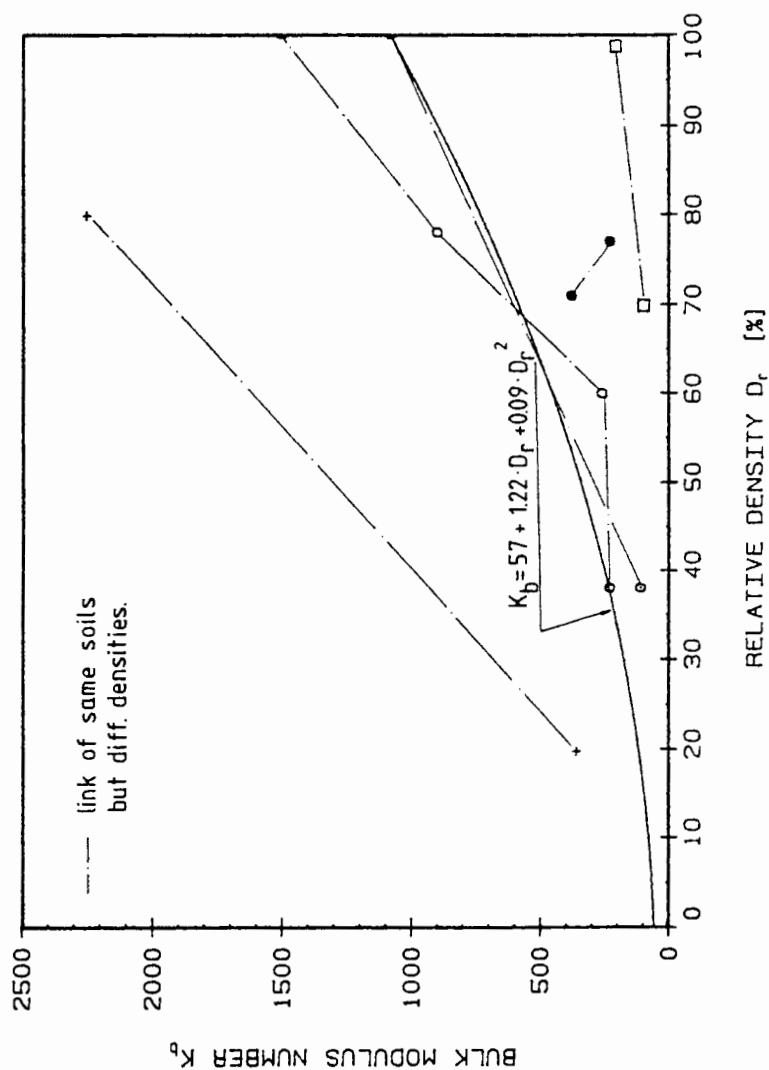


Figure 16. Bulk Modulus Number K_b as a Function of Relative Density.

in all cases is increasing with density. The relationship is given by Eq. 3-22.

$$K_b = 57 + 1.22 \cdot D_r + 0.09 \cdot D_r^2 \quad (3-22)$$

The relative density is also used in %. Backcalculation of the bulk modulus parameters for most cases, including Willamette River sand, which have not been included in the correlation procedure gave reasonable results.

CONVENTIONAL PARAMETERS

The cohesion and friction parameters are the traditional properties presented in Chapter II. Since this study is confined to granular soils i.e. sands, silts and gravels, which rely entirely on friction for the mobilisation of shear strength, only ϕ and $\Delta\phi$ are of significance.

Conventional Parameters from PMT

The pressuremeter test is fundamentally different from conventional soil investigation methods, so the different set of soil parameters is not surprising. It is apparent however, that the use of these parameters is most likely to yield the best results. Nevertheless, correlations of pressuremeter data to conventional parameters have been reported (G.Y. Felio, J.-L. Briaud, 1986) and used with success.

C.P. Wroth (1982) recommended the use of the following equations.

$$\sin \phi' = \frac{(K_a + 1) \cdot s}{(K_a - 1) \cdot s + 2} \quad (3-23)$$

$$\sin \theta = \frac{2K_a s - (K_a - 1)}{(K_a + 1)} \quad (3-24)$$

$$s = \frac{\sin \phi' \cdot (1 + \sin \Theta)}{(1 + \sin \phi')} \quad (3-25)$$

where ϕ' is the effective angle of internal friction, Θ is the angle of dilation, and K_a is the active earth pressure coefficient as given by Eq. 3-26.

$$K_a = \tan^2 \left(\pi/4 + \phi_{cv}/2 \right) \quad (3-26)$$

and ϕ_{cv} is the angle of internal friction at the end of the pressuremeter test at which the sand has reached its critical state. C.P. Wroth (1982) states that if ϕ_{cv} is unknown it might be approximated by $\phi_{cv} = 35^\circ$.

Recognizing that the angle of repose for a granular material is equal to the angle of internal friction at the critical void ratio (constant volume) D.H. Cornforth (1973) recommended the use of a diagram (Fig. 17) in which the increase in ϕ' is given as a function of the relative dry density. The actual value for ϕ' is calculated using Eq. 3-27.

$$\phi' = \phi_{cv} + \phi_{dc} \quad (3-27)$$

An empirical correlation between the practical net limit pressure, p_1^* , and the angle of internal friction has been published (Centre d'Etudes Ménard, 1978).

$$\phi' = 5.77 \cdot \ln(p_1^*) - 7.86 \text{ (kPa)} \quad (3-28)$$

COMPONENTS OF STRENGTH AS A FUNCTION OF DENSITY

AFTER: D.H. CORNFORTH (1973)

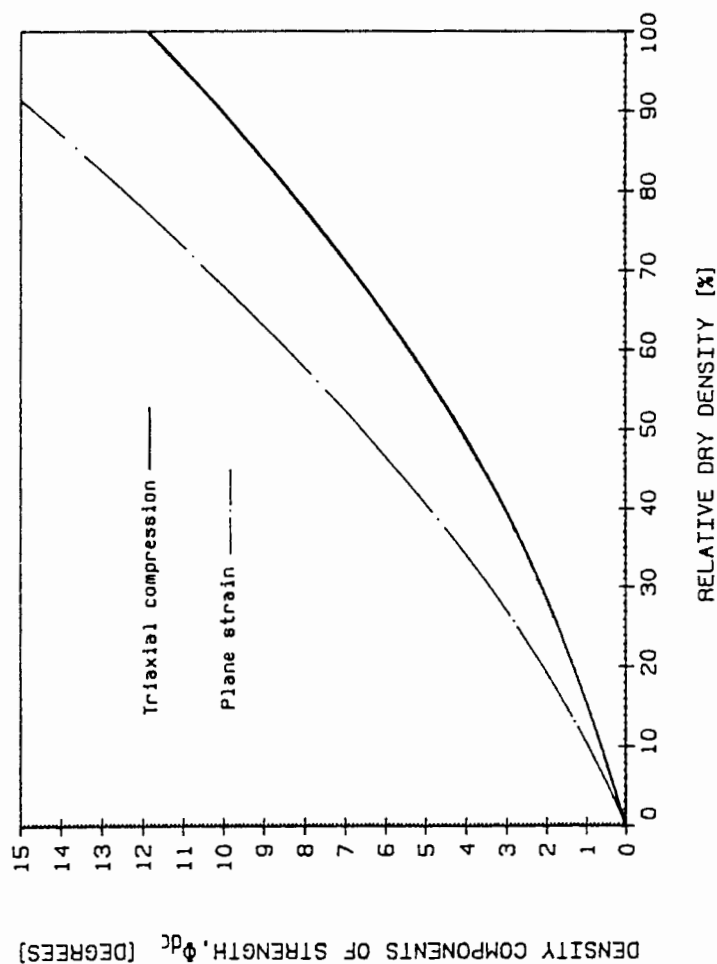


Figure 17. Density Components of Strength ϕ' .

Finally, it should be noted that, using Eqs. 2-13, 2-14 and others a theoretically correct value for ϕ could be calculated if c is known. It has been shown (F. Baguelin, J.F. Jezequel and D.H. Shields, 1978) however, that minor errors in σ_f , p_0 and p_1 have a significant impact on the computed angle of internal friction. The accumulation of those errors might even lead to meaningless results, so that this approach can not be recommended.

For the calculation of initial stresses due to gravity, the lateral earth pressure coefficient at rest, K_0 , and the dry unit weight, γ_{dry} , is also a frequently required input for finite element programs.

K_0 is defined as the ratio of the horizontal effective stress, σ_h' , to the effective vertical stress, σ_z' .

$$K_0 = \frac{\sigma_h'}{\sigma_z'} \quad (3-29)$$

Theoretically, p_{0M} as shown in Fig. 4, should give some indication of the value of K_0 , because it indicates the point on the pressuremeter curve where the soil has been reloaded to its initial stress state. However, unavoidable borehole disturbance and membrane resistance have a strong impact on this early part of the pressuremeter test, so that K_0 and γ_{dry} are usually assumed, based on soil type and condition or other soil tests.

T.C. McCormack (1987) showed in a parametric study for

a retaining wall that K_0 has only negligible effects and hence, it seems reasonable to base K_0 and γ_{dry} on engineering judgement. Typical values for various soil types can be found in virtually any soil mechanics textbook.

CHAPTER IV

SOIL TESTING PROGRAM

SELECTED SOIL

All tests were conducted using dry Willamette River sand containing grains of subangular shape. The grain size distribution curve is given in Fig. 18. According to the unified system of soil classification, the sand is classified as SP. The specific gravity was determined as 2.70, the minimum and maximum densities were 1.30 g/cm^3 and 1.67 g/cm^3 , respectively. The angle of repose was found to be $\phi_{cv} = 31.9^\circ$.

A total of twelve direct shear tests with normal stresses ranging from 15.5 kPa to 124 kPa were carried out. Furthermore, three pressuremeter tests at two different depths, as well as nine triaxial compression, tests were conducted.

TRIAXIAL TESTS

A total of nine consolidated-drained triaxial compression tests were carried out at confining pressures of 138 kPa, 276 kPa, and 414 kPa. Failure was approached at a constant rate of strain. Three test series in relative densities of 50 %, 70 %, and 95.6 % were conducted. Since

Grain Size Distribution [mm]

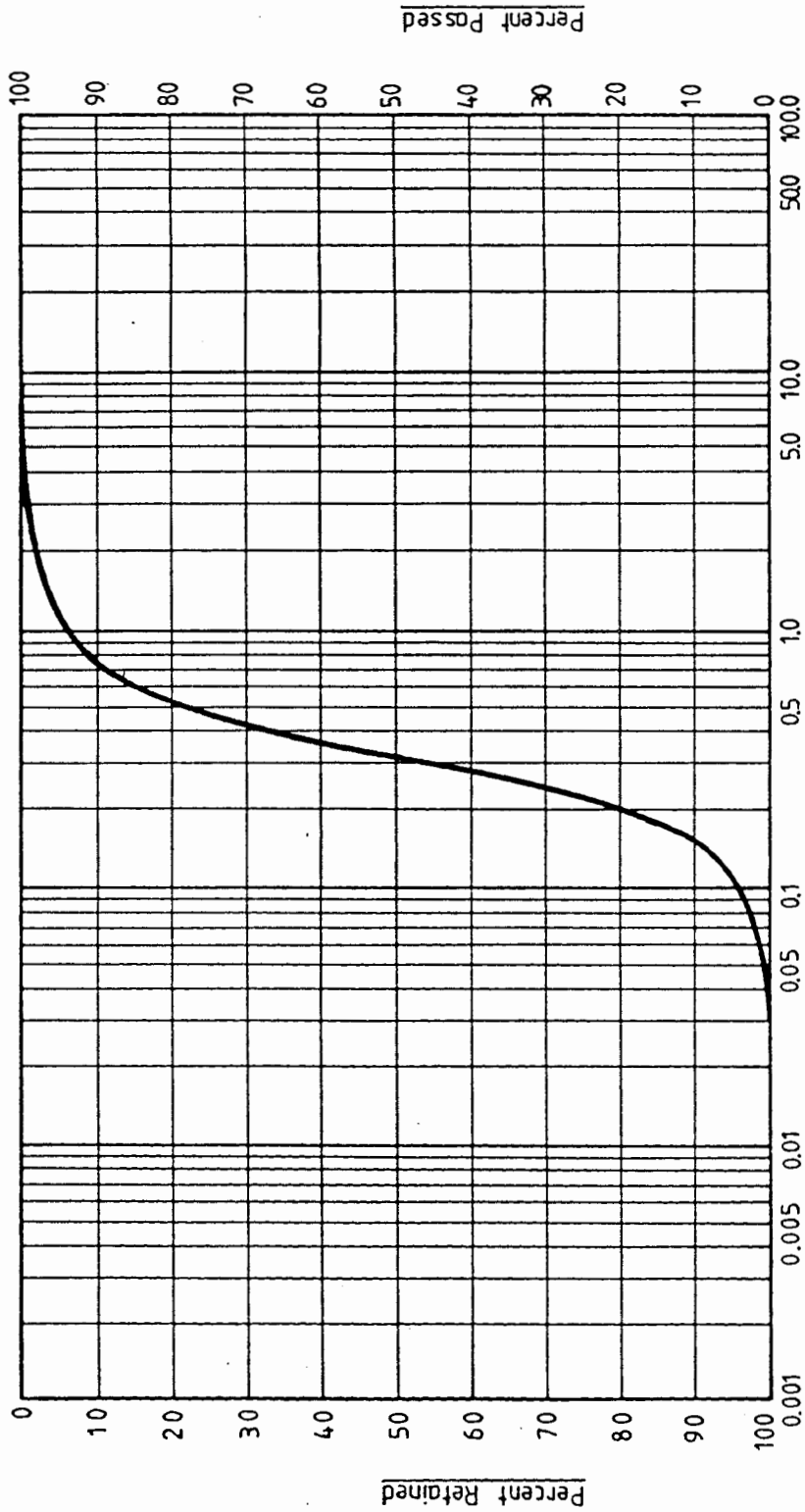


Figure 18. Grain Size Distribution Curve
for Willamette River Sand.

volume changes are an important aspect of the triaxial tests a large specimen size of 7.2 cm diameter and 14 cm height was chosen, thus magnifying poisson's ratio effects. The specimen ends were not lubricated.

Sample Preparation

It is virtually impossible to obtain undisturbed sand specimens for triaxial tests, but since the accompanying pressuremeter tests were conducted in an artificially placed soil it is now possible to reconstruct samples of equal, or at least similar, properties.

Two rubber membranes inside each other were mounted in a membrane jacket, a slight vacuum was applied and a porous stone fitted inside the membrane, forming the bottom of the sample and allowing for drainage. The membrane jacket was arranged on the pedestal and a predetermined amount of sand, corresponding to the desired density, was placed uniformly inside the membrane and topped with a second porous stone.

Whithout releasing the vacuum stretching the membranes, the inner membrane was slid over the top cap. The application of a slight internal negative pressure through a hole in the pedestal added some strength to the sample, so that the outer membrane and the O-rings could be slid over the top cap and the external support by the membrane jacket therefore made redundant. From that point on the standard procedure to assemble the confining chamber and the dial

gauges was followed. A confining pressure of 34 kPa was applied before the internal negative pressure was released. Hence, the specimen had never been without support or confinement.

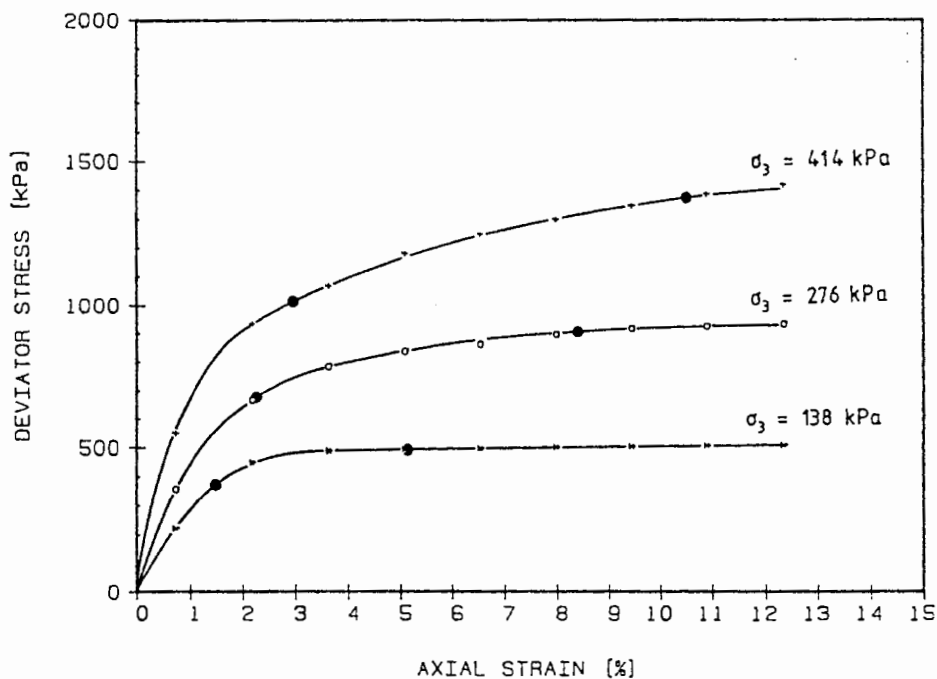
Prior to testing, the specimen was saturated in order to observe volume changes and the confining pressure was increased to the test level. After sufficient time for the sample to consolidate under the all around confining pressure (depending on the specimen density and the confining pressure it took from 15 to 30 minutes) the test was conducted.

Failure to seal the sample effectively would have resulted in erratic volume change measurements, therefore a high vacuum grease was used to establish, and maintain, the best possible contact between the pedestal or top cap and the membrane. The use of two membranes and two O-rings for each end added further to the seal quality.

Test Results

Volume change and axial load readings were taken every 0.051 cm of deformation, corresponding to 0.36 % axial strain. For the first test ($D_r = 50\%$ and $\sigma_3 = 138$ kPa) twice as many data points, as for the remaining tests, were recorded. The data points given in the following diagrams represent the genuine material properties. Stress-strain diagrams with volume change curves of the tests are given in Fig. 19, 20, and 21. A correction for membrane resistance,

STRESS-STRAIN CURVES



TRIAXIAL TESTS - $D_r = 50\%$

VOLUME-CHANGE CURVES

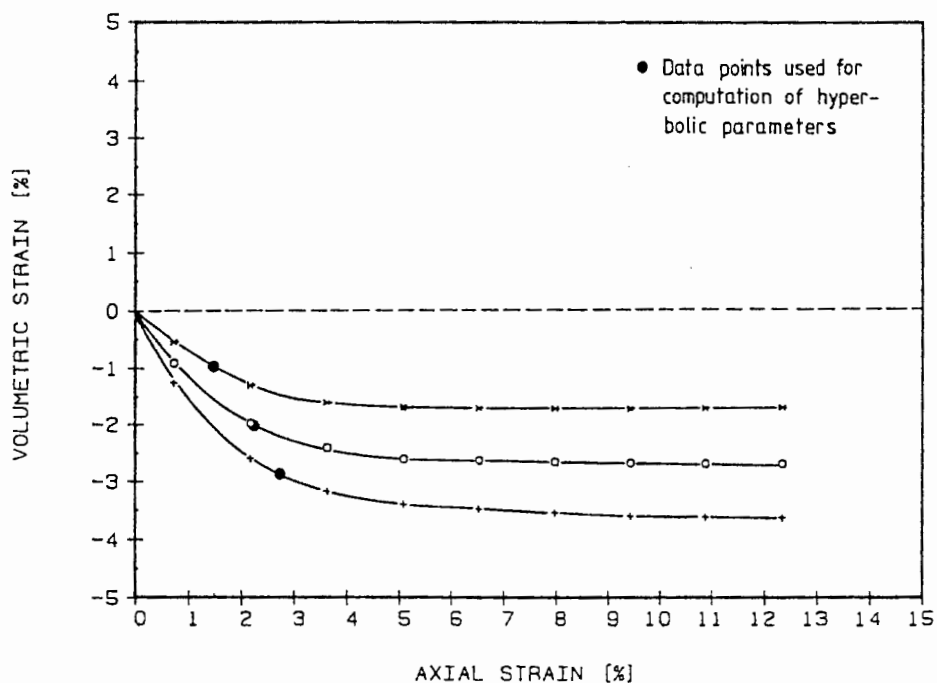
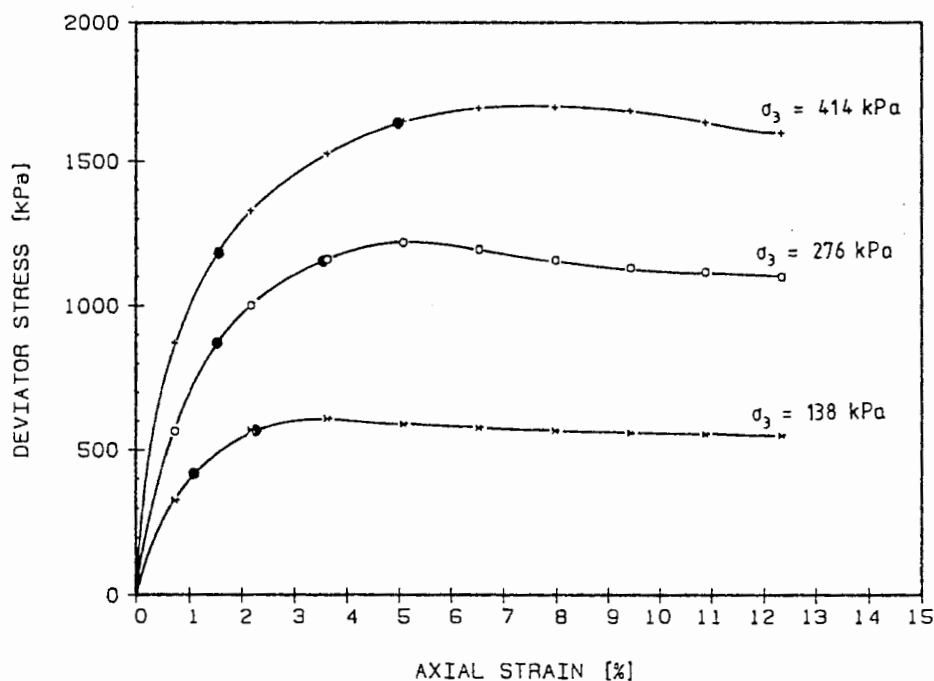


Figure 19. Stress-Strain and Volume Change Curves for Willamette River Sand, $D_r = 50\%$.

TRIAXIAL TESTS - $D_r = 70\%$

STRESS-STRAIN CURVES



TRIAXIAL TESTS - $D_r = 70\%$

VOLUME-CHANGE CURVES

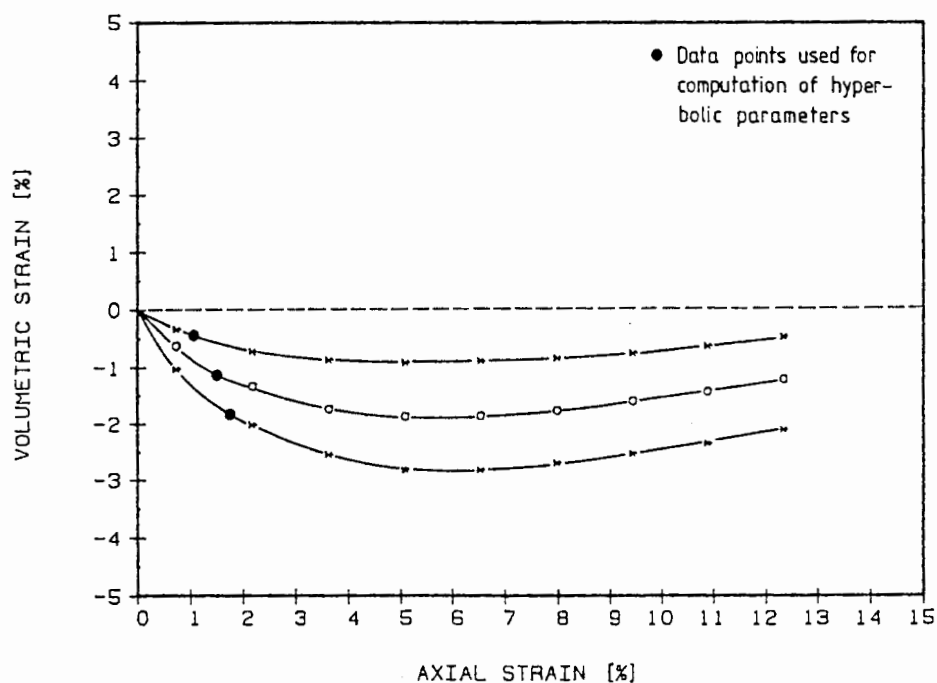
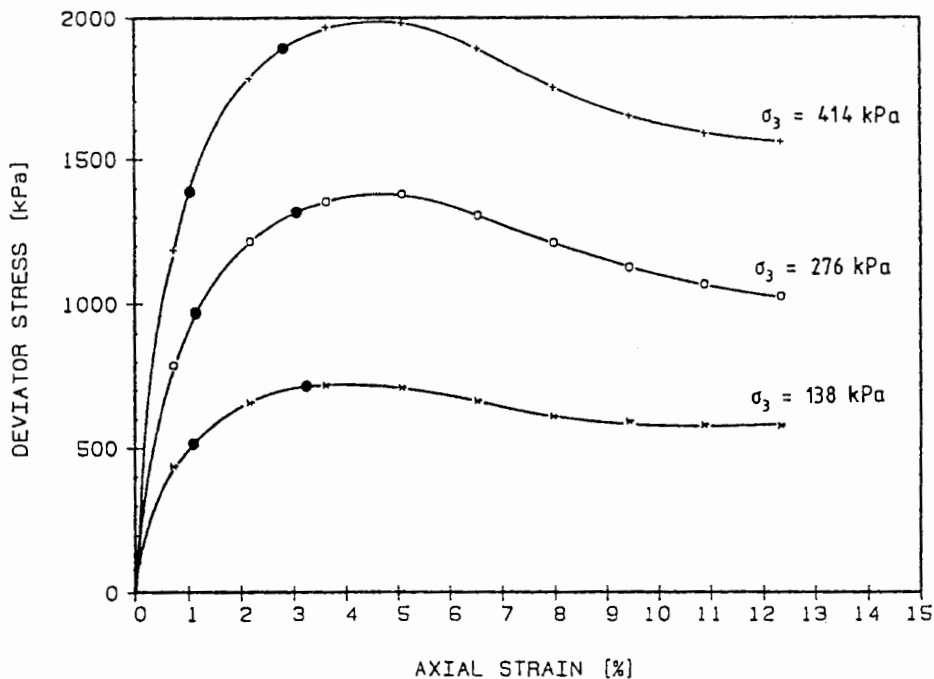


Figure 20. Stress-Strain and Volume Change Curves for Willamette River Sand, $D_r = 70\%$.

STRESS-STRAIN CURVES



TRIAXIAL TESTS - $D_r = 95.6\%$

VOLUME-CHANGE CURVES

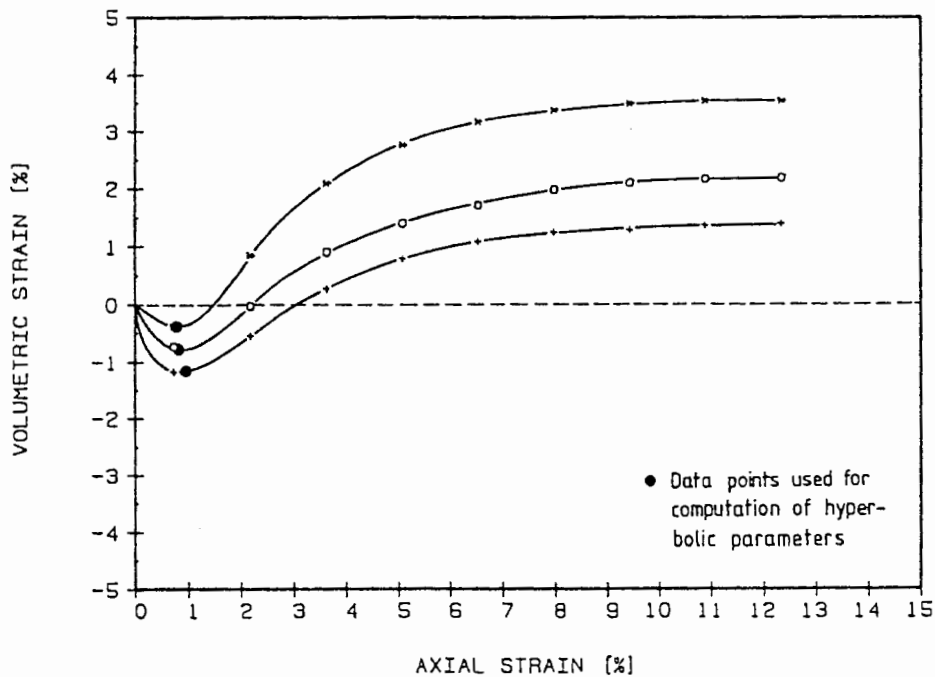


Figure 21. Stress-Strain and Volume Change Curves for Willamette River Sand, $D_r = 95.6\%$.

drain resistance or ram friction was neglected, and it is not done on a routine basis with these test rates.

Table II summarizes the hyperbolic soil parameters computed in accordance with the soil model by J.M. Duncan (1980), as presented in Chapter III. Sample calculations are given in the Appendix.

The finite element code AXISYM requires poisson's ratio values prior to, and at, failure as input and avoids the bulk modulus formulation. Using Eqs. 3-6 and 3-19 values corresponding to the computed bulk modulus parameters have been determined and are listed for completeness. Since failure for the higher densities coincides with horizontal tangent moduli, a value of 0.5 would be appropriate. The same value is chosen for the lower density because no volume change takes place when the critical void ratio is reached. Due to limitations of the finite element formulation a value of $\nu_f = 0.49$ has been selected.

TABLE II
PARAMETERS FOR SAND - HANDCALCULATED

Parameter	$D_r = 50 \%$	$D_r = 70 \%$	$D_r = 90 \%$
K	540	650	860
n	0.45	0.65	0.95
ϕ	39.5	40.7	43.7
R_f	0.91	0.78	0.86
K_b	106	315	360
m	0.19	0.05	0.0
ν	0.33	0.39	0.30
ν_f	0.49	0.49	0.49

The computer program SP-5 written by Kai Wong at the University of California at Berkeley in 1977 (J.M. Duncan et al. 1980) , was adopted to evaluate the strength and stress-strain parameter by means of the least squares regression method. The computer solutions for the conducted triaxial tests are given in the Appendix.

Comparision of the computed bulk modulus values with the proposed correlation to relative density, as displayed in Fig. 15 and 16, reveals only little deviation from the given curve. So that the incorporation of the Willamette River sand data would not have changed the correlation significantly.

Good agreement to hand computed values is recognized upon inspection of Table III, which summarizes the parameter obtained by the computer program. The increased deviation for the bulk modulus numbers with increasing density is believed to be a result of the deviator stresses used by the program to compute the bulk moduli.

TABLE III
PARAMETERS FOR SAND - SP-5 SOLUTIONS

Parameter	$D_r = 50 \%$	$D_r = 70 \%$	$D_r = 90 \%$
K	555	645	872
n	0.43	0.78	0.93
ϕ	39.8	41.0	44.0
R_f	0.91	0.78	0.85
K_b	104	298	396
m	0.17	0.04	0.0
ν	0.33	0.39	0.30
ν_f	0.49	0.49	0.49

PRESSUREMETER TESTS

An EX PUP pressuremeter with a monocell probe (32 mm diameter) and a length to diameter ratio of $L/D = 8$ was used for all tests. The control unit was located at an elevation not requiring any hydrostatic correction at the gauge level. The pressuremeter was placed in the soil container prior to deposition to eliminate stability problems from the dry sand. A total of three pressuremeter tests were carried out.

Placement Procedure

Pressuremeter testing took place in a plywood, cube-shaped chamber 90 cm x 90 cm x 90 cm, and in steel drums of 57 cm diameter and a height of 86 cm. The sand, air dried (water content = 1.0 %), was deposited by pluviation through air from a constant height of fall of 90 cm through openings of 20.6 mm and 14.3 mm in diameter, resulting in a uniform, relative density of $D_r = 68$ %. Density pots were placed during deposition of the sand and penetration tests were carried out to confirm the desired uniformity. Further details of the sample preparation have been described by J.J. Kolbuszewski and R.H. Jones (1961) and by T.D. Smith (1983).

Test Results

Injected volume and radial pressure readings were taken every 10.1 cm³ of injected volume corresponding to

4.63 % of volumetric strain. The first test was performed in the plywood chamber and the following two in the steel drums. Equal test results for the chamber test and the first drum test (both were conducted under equal overburden pressure) confirm that the different sizes of the testing container did not influence the test results, but the amount of sand to be deposited had been reduced considerably.

For volume loss and membrane resistance corrected, pressuremeter curves are given in Fig. 22 - 24. Their different appearance from the typical pressuremeter curve, as given in Fig. 4, is expected considering that the probe was in place while the sand was deposited. For this reason no stress relief took place in order to drill the hole for probe insertion and therefore the curves are similar in shape to those from selfboring pressuremeter tests. The interpretation of the curves however, is essentially identical.

The problem of a critical depth, D_c , for pressuremeter tests has been investigated by a number of researchers. J.-L. Briaud and D.H. Shields (1981) reported critical depth effects on the limit pressure up to a depth of 20 diameters or 1.20 m in medium dense to dense sands. Deformation moduli were not influenced. A finite element study by T.D. Smith (1983) indicates a critical depth for cavity moduli at approximately 12 times the radius of the probe.

Considering the foregoing, the pressuremeter curves

PRESSUREMETER TEST - CHAMBER I

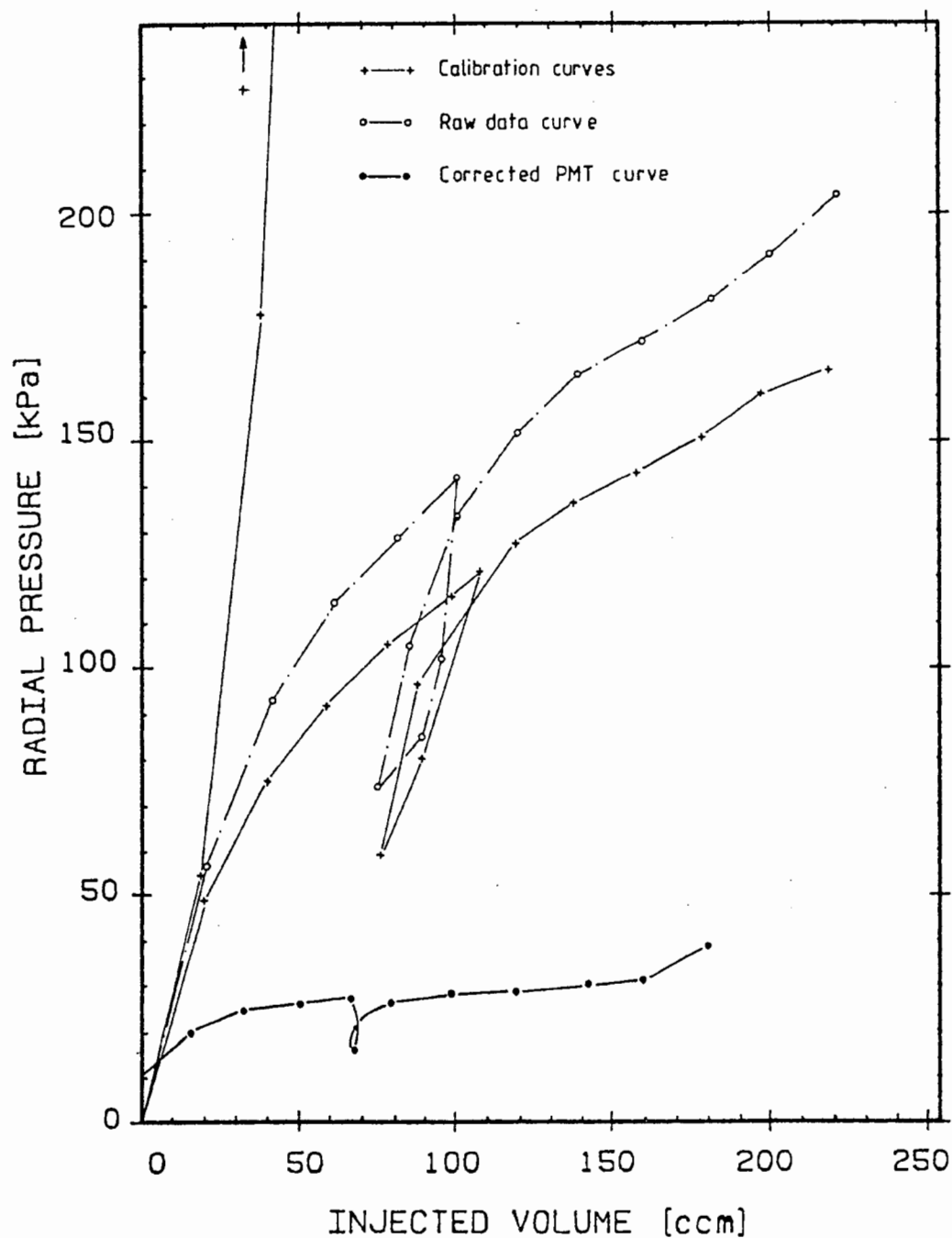
 $D_r = 66.4 \%$, Depth = 57 cm

Figure 22. Pressuremeter Curve - Chamber Test, $D_r = 66 \%$.

PRESSUREMETER TEST - DRUM I

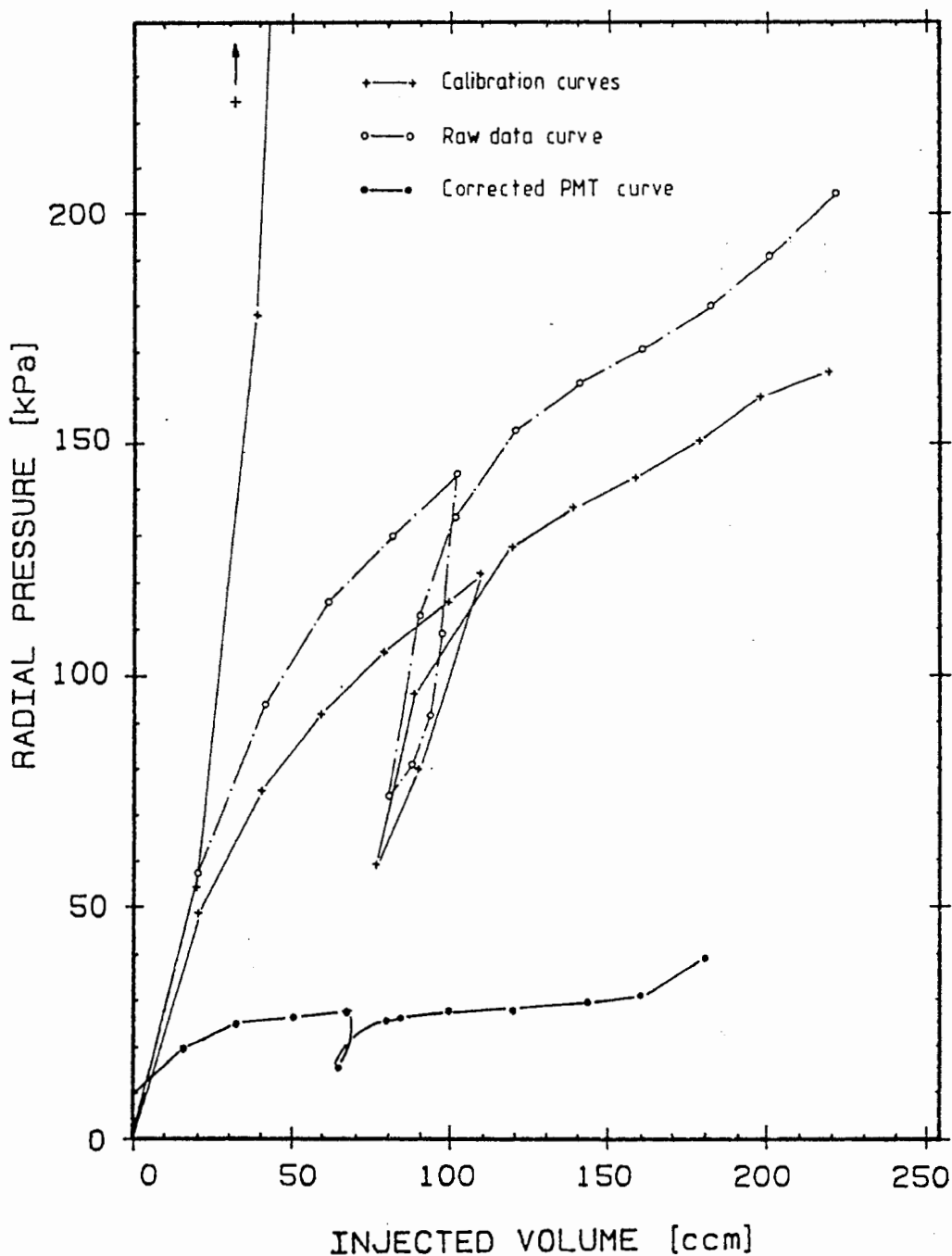
 $D_r = 66.9 \%$, Depth = 57 cm

Figure 23. Pressuremeter Curve - Drum Test I, $D_r = 67 \%$.

PRESSUREMETER TEST - DRUM II

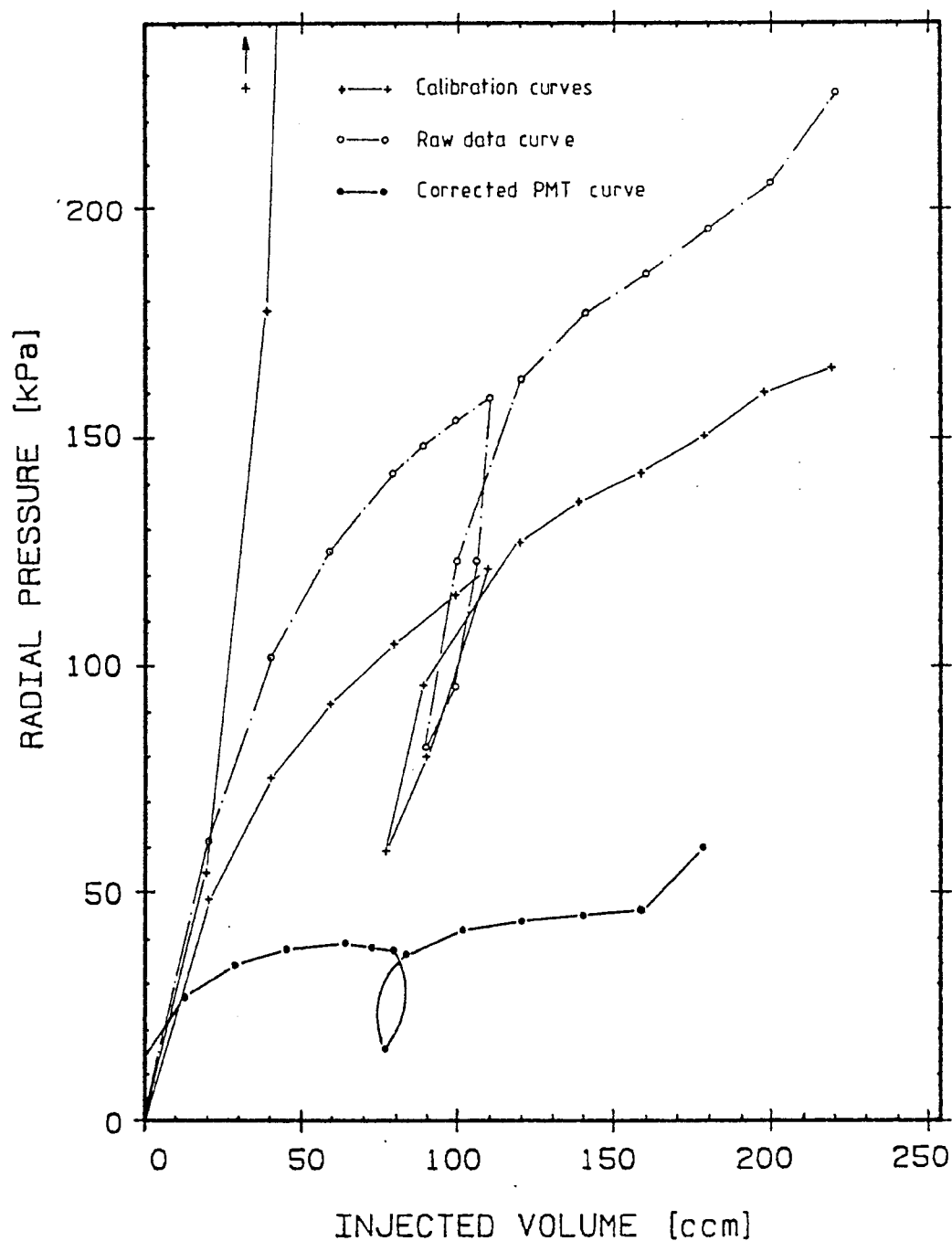
 $D_r = 67.9 \%$, Depth = 147 cm

Figure 24. Pressuremeter Curve - Drum Test II, $D_r = 68 \%$.

given in Fig. 22 and 23 are probably influenced by critical depth effects and have to be carefully inspected. Even though the data reduction for drum test 11 (Fig. 24) has been difficult due to low confining pressures and a high membrane resistance the given curve most likely represents the genuine material properties.

The following soil parameters are computed according to the proposed method and are summarized in Table IV based on the pressuremeter tests illustrated in Fig. 23 and 24.

TABLE IV
PARAMETERS FOR SAND BASED ON PRESSUREMETER TESTS

Parameter	$D_r = 68 \%$
K_{PM}	84 (650) *
s	0.51 (0.65) *
ϕ	41.9 (40.7) *
R_f	0.71 (0.78) *
K_b	556 (315) *
m	0.09 (0.05) *
ν	0.33 (0.39) *
ν_f	0.49 (0.49) *

* Based on triaxial data (see also Table II).

CHAPTER V

FINITE ELEMENT STUDIES

INTRODUCTION

The finite element method has, since its development by M.J. Turner et al. (1956), experienced an enormous number of applications in many engineering disciplines. In principle, a continuum is divided into discrete elements with connecting nodal points and equilibrium equations are generated for each element with unknowns at each nodal displacement. These equations are stored in matrix form and solved for the nodal displacements. Once the joint displacements are known the strains and subsequently the stresses within each element can be calculated from elasticity.

The stress-strain relationship for axisymmetric solids, expressed in Eq. 5-1, is based on the generalized Hooke's law and applies to each element, the solution is obtained for the entire continuum.

$$\begin{bmatrix} \sigma_r \\ \sigma_z \\ \sigma_\theta \\ \tau_{yz} \end{bmatrix} = \frac{E}{(1+\nu)(1-2\nu)} \cdot \begin{bmatrix} 1-\nu & \nu & \nu & 0 \\ \nu & 1-\nu & \nu & 0 \\ \nu & 1-\nu & \nu & 0 \\ 0 & 0 & 0 & \frac{1-\nu}{2} \end{bmatrix} \cdot \begin{bmatrix} \epsilon_r \\ \epsilon_z \\ \epsilon_\theta \\ \gamma_{yz} \end{bmatrix} \quad (5-1)$$

It is apparent that this solution procedure is only practicable in conjunction with high speed computers in order to solve for the many unknowns in the large number of equations. In fact, a fairly simple structure, consisting of only a few elements, could not be solved by hand.

In the case of most geotechnical finite element codes, the nonlinear behavior of the material compounds the complicated process with the difficulty of updating modulus of elasticity values, depending on the current stress level. Furthermore, anisotropy, dilatancy (granular soils), strain softening (brittle materials) as well as time dependency and stress history are factors of significant influence on soil displacements upon load application. This wide variety of problems illuminates the enormous difficulties to formulate a general constitutive law for soils.

The implementation of the hyperbolic soil model into computer programs employing the finite element method was the next logical step after its initial formulation by F.H. Kulhawy et al. (1969). Since then this model has been linked to numerous finite element programs for the solution of various geotechnical problems.

FINITE ELEMENT PROGRAM "AXISYM"

The finite element program AXISYM developed by D.M. Holloway (1976) models the nonlinear behavior of the soil according to a hyperbolic function (described in

Chapter III except for the bulk modulus formulation) incrementally in successive, linear portions (Fig. 11).

In solving the finite element mesh for its nodal displacements, a distinct tangent modulus value is assigned to each of the five node (four external and one internal) quadrilateral elements depending on the current stress level in the specific element. In other words, a linearly elastic program is tricked into nonlinear modelling by a piecewise linear elastic solution of a nonlinear problem. The principal advantage of the tangent modulus approach rather than utilizing the secant modulus is, that a non-zero stress state can be modelled. In addition, a full load vs. deflection response is obtained.

In addition to the aforementioned two-dimensional element, the use of a one-dimensional interface element is possible to allow relative displacements between two solid elements. The problem geometry and loading conditions are modelled in axisymmetric coordinates. Loads may be applied in steps and additional iterations can be specified to improve convergence. The assigned tangent modulus is updated and subsequently the mesh is solved again for its nodal displacements, strains and stresses.

It should be noted that the stress-strain relationship given by Eq. 5-1 is accurate only in the range of small strains and therefore only stresses and strains prior to failure should be considered.

Volume Changes

In the formulation of AXISYM, the latest version of the hyperbolic soil model is not incorporated, i.e. the bulk modulus formulation is omitted. Two values of poisson's ratio are required as part of the material property input, this is poisson's ratio before failure and at failure, ν_f . Clearly, poisson's ratio is constant regardless of the stress level up to failure, from whereon the second value is used.

Problems due to a value of ν approaching 0.5 can be seen by inspection of the term preceeding the elasticity matrix (Eq. 5-1). The solution of the matrix for radial, circumferential, axial and shearing strains would cause an unstable situation. Plane strain and axisymmetric problems encounter in this respect similar difficulties for constant volume or dilatant soils and most geotechnical problems are frequently grouped into either of these two categories.

For these reasons, both values of ν are not to exceed the specified limits of

$$0 < \nu < 0.49 \quad (5-2)$$

This implies that dilatant materials like dense sands or stiff clays with values of $\nu > 0.5$ can not be modelled accurately, which is somewhat less critical since the hyper-

bolic model itself does not account for dilatancy.

Noteworthy is the approach L.R. Herrmann (1965) took, in his entirely different stress-strain relationship formulated for elastic materials. The problems due to $\nu = 0.5$ are eliminated.

FINITE ELEMENT ANALYSIS - PRESSUREMETER TEST

To evaluate the computed hyperbolic soil parameters and in order to gain an increased understanding of the soil behavior during cavity expansion, a pressuremeter test was simulated analytically using the finite element code AXISYM. The accuracy of the code was evaluated by a "patch" test as recommended by R.H. MacNeal and R.L. Harder (1984). A thick walled cylinder with elastic properties and an internal pressure condition was analyzed. Good agreement to the close form solution was observed with a deviation of -8 % to the handcomputed values if poisson's ratio was taken as 0.49. The validity of the chosen mesh with 260 elements, as displayed in Fig. 25, was confirmed using the elastic solution by M. Livneh et al. (1971).

Two materials were used for the nonlinear AXISYM analysis. The soil was Willamette River sand with 70 % relative density for which the hyperbolic parameters have been determined in Chapter IV. The second material was an elastic material simulating drilling fluid, and supported the cavity during gravity-turn-on prior to pressure application. Table V summarizes the selected parameters.

Figure 25. Finite Element Mesh for Analysis of Pressuremeter Test.

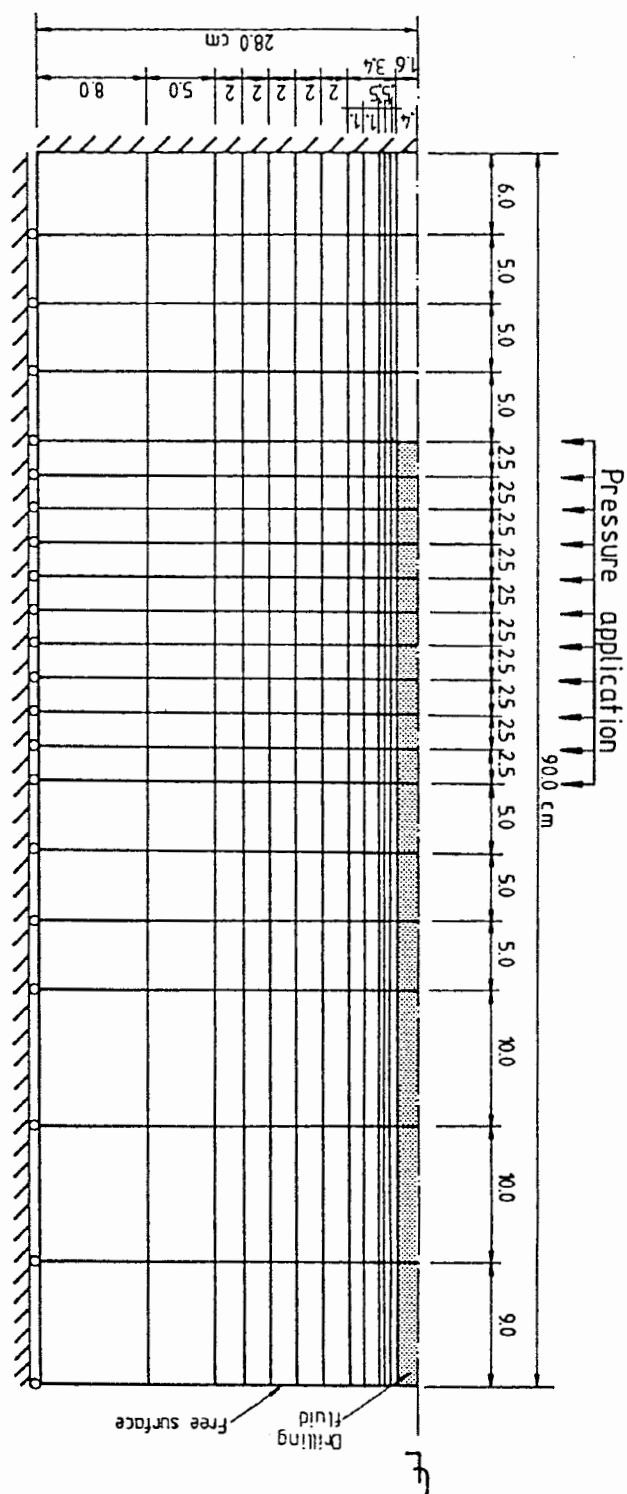


TABLE V
 TRIAXIAL SP5-PARAMETERS USED FOR ANALYSIS OF PMT

Parameter	Willamette River Sand	Drilling Fluid
K	645	1.0
n	0.78	0.0
ϕ	41.0	0.0
R_f	0.78	1.0
ν	0.39	0.20
ν_f	0.49	0.20
K_0	0.4	1.0
γ_{dry}	15.10 kN/m ³	23.70 kN/m ³

An increasing hydrostatic pressure was applied from within the cavity. The computed displacements allowed the calculation of the corresponding cavity volume. Additional analysis with the same parameters but a vertically expanded mesh, allowed the simulation of pressuremeter tests at varying confining pressures. A plot of the computed soil moduli with increasing depth (Fig. 26) confirms the relationship given in Chapter III, proposed for a variation of pressuremeter moduli with overburden pressure. The absolute number however, is different from the actually measured value as displayed in Fig. 26, indicating a possible violation of the fundamental plane strain assumption.

SOIL MODULUS AS A FUNCTION OF DEPTH BASED ON AXISYM SOLUTIONS AT $\epsilon_\theta = 5\%$

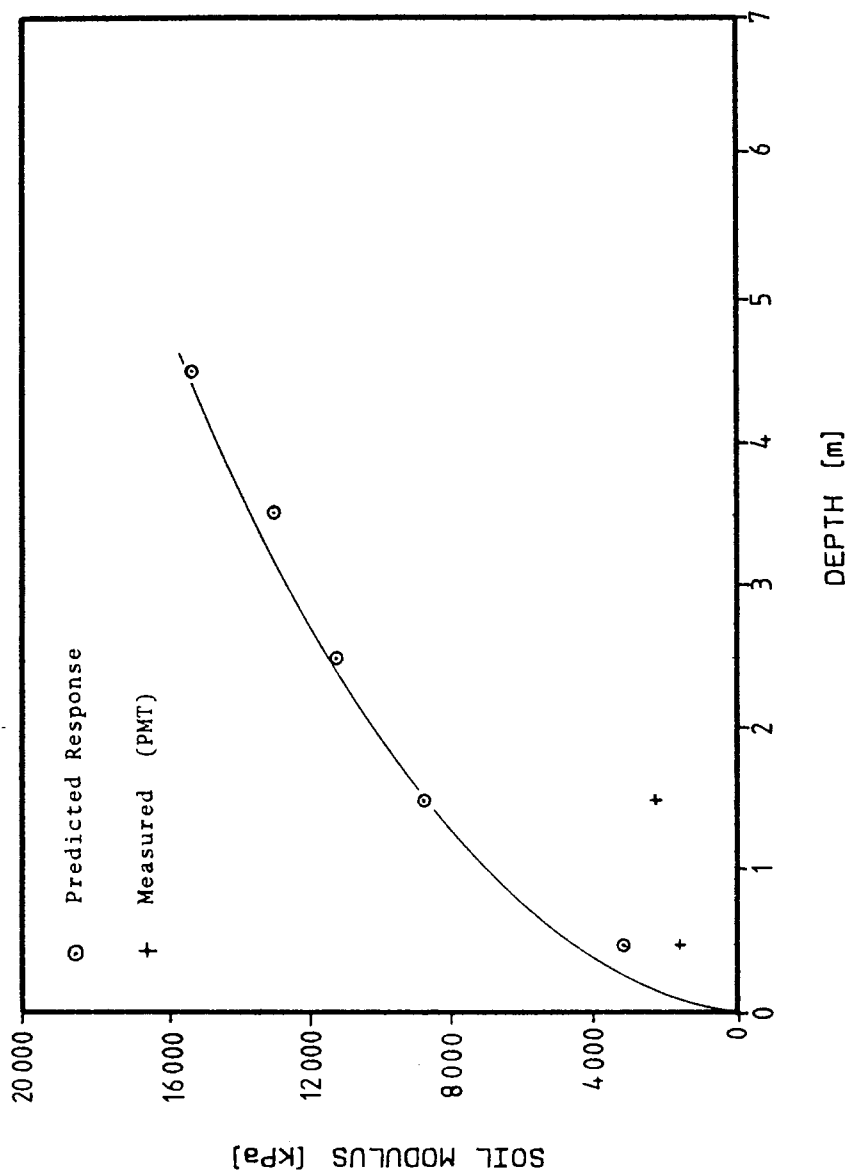


Figure 26. Variation of Pressuremeter Moduli with Increasing Depth.

FINITE ELEMENT ANALYSIS - FOUNDATION

The first independent use of the hyperbolic parameters based on pressuremeter testing was made by predicting the load deflection response of a circular footing, with similar characteristics as the model foundation in the following chapter.

The vertical surface displacement for a rigid circular foundation on elastic material is given (H.G. Poulos and E.H. Davis 1974) by,

$$\delta_z = \pi/2 \cdot (1 - \nu^2) \cdot \frac{P_{av}a}{E} \quad (5-3)$$

where P_{av} is the average pressure acting on the soil and 'a' is the radius of the loaded area. Using elastic properties an AXISYM analysis gave almost identical results compared to the close form solution (deviation -2 %).

Modelling the problem analytically, using the finite element program AXISYM, a center point load of 100 N was applied in 19 increments. A total of four different materials was used to simulate the mesh configuration as presented in Fig. 27. The same soil was used with a relative density of 70 %, for which the previously calculated hyperbolic parameters from pressuremeter testing were used. Average properties for brass were assigned to the elements representing the foundation. A row of one-dimensional interface elements has been introduced between the

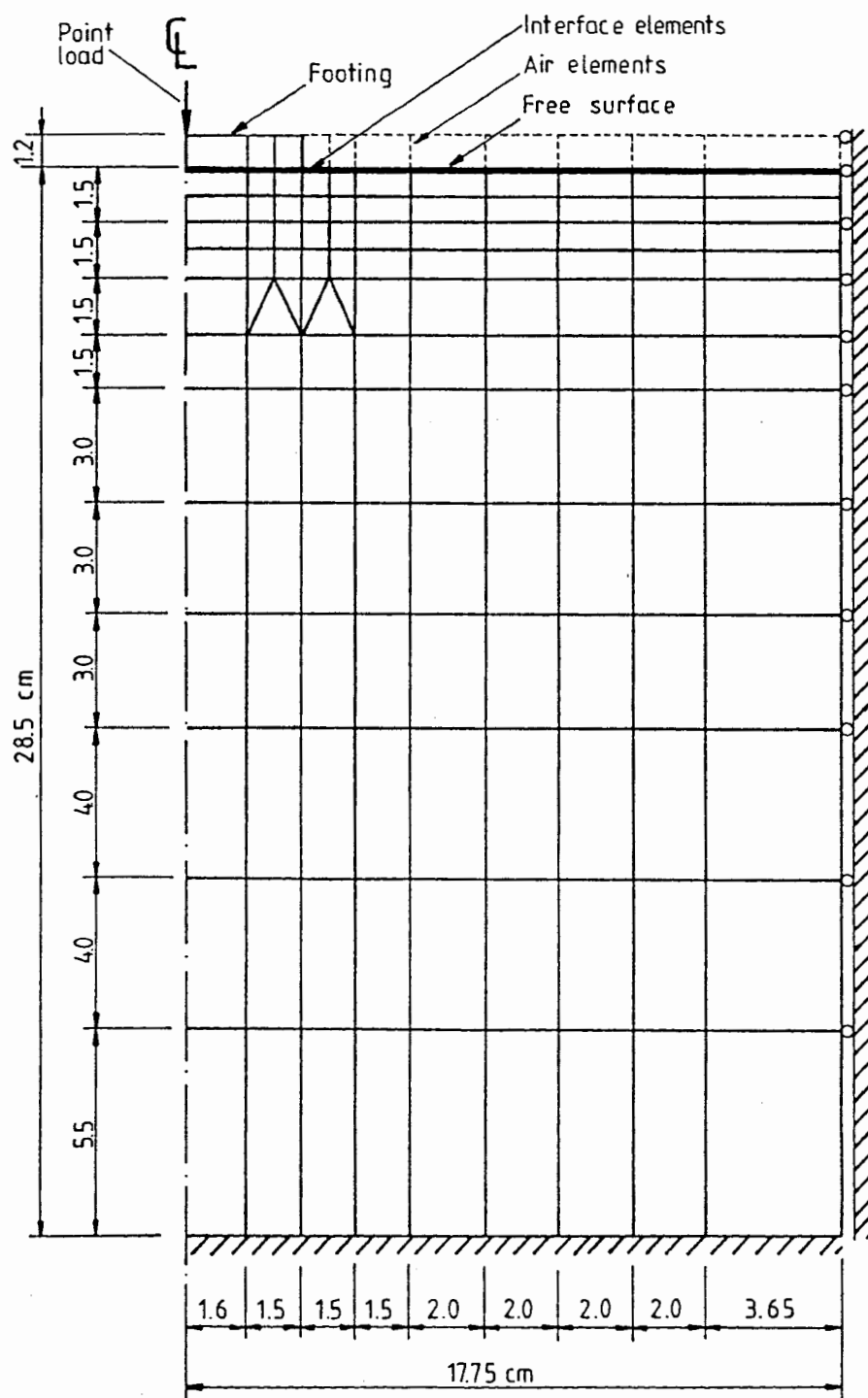


Figure 27. Finite Element Mesh for Analysis of Model Foundation.

foundation base and the soil surface to permit slip between the two materials. Finally, elements having the properties of air have been employed to form a continuum. Table VI summarizes the selected values.

The mesh containing 142 elements was analyzed in axisymetry. The introduction of the interface elements did not yield significant changes in displacements or stresses. The performance of the foundation in terms of settlements at the footing center vs. axial load is presented in Fig. 28.

TABLE VI
PRESSUREMETER PARAMETERS USED FOR FOUNDATION ANALYSIS

Parameter	Willamette River Sand	Foundation (brass)	Interface Element
K	84	0.0	1500
n	0.51	0.0	0.8
ϕ	41.9	0.0	$\delta = 25^\circ$
R_f	0.71	1.0	0.8
ν	0.33	0.30	-
ν_f	0.49	0.30	-
K_0	0.40	0.0	-
γ_{dry}	15.10 kN/m ³	118.81 kN/m ³	-

ANALYTICAL FOUNDATION RESPONSE BASED ON AXISYM SOLUTIONS

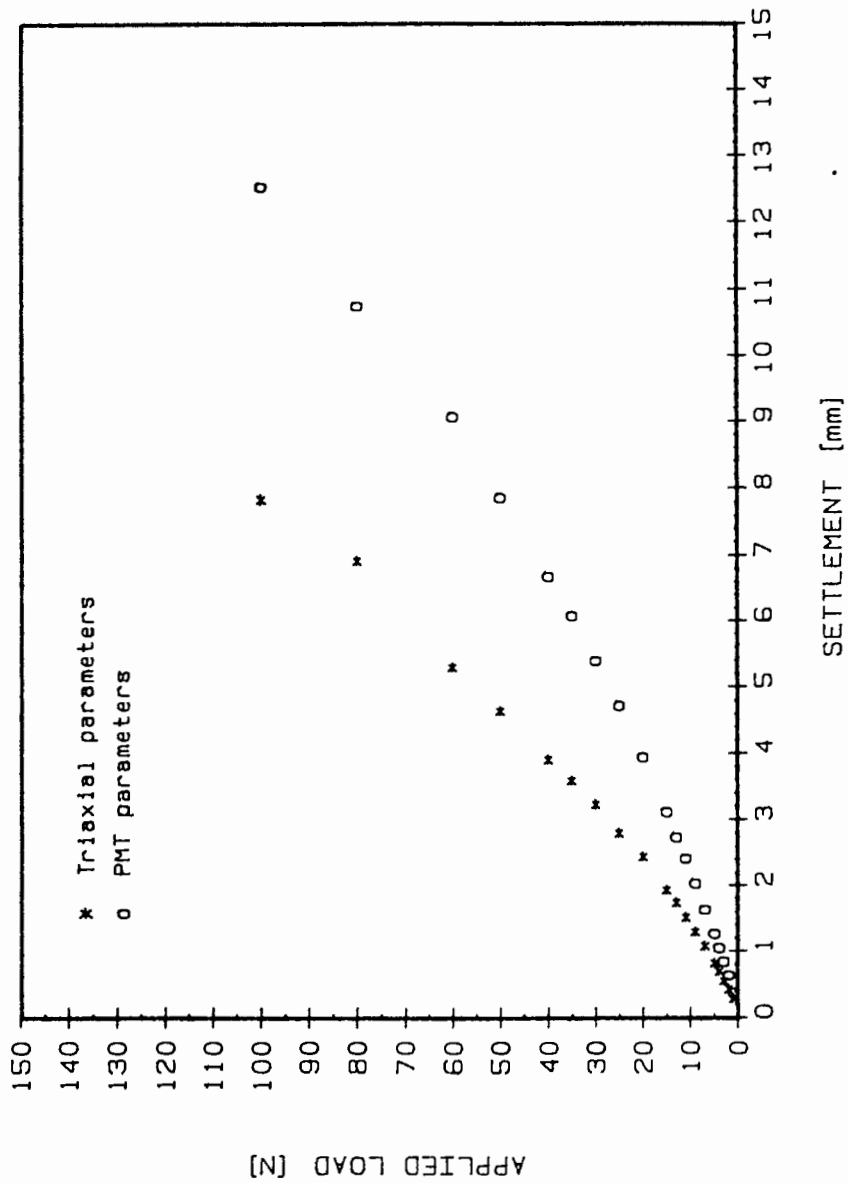


Figure 28. Load-Deflection Response for Model Foundation from AXISYM using Pressuremeter Parameters.

A detailed inspection of the accumulated computer results revealed a very clear picture of the generated failure mechanisms. From the first load application of 1 N failure was noticed in some of the elements. Initiating from the footing edges failure continuously extended into the halfspace upon load increase. Graphically the load failure relationship for the elements is captured in Fig. 29.

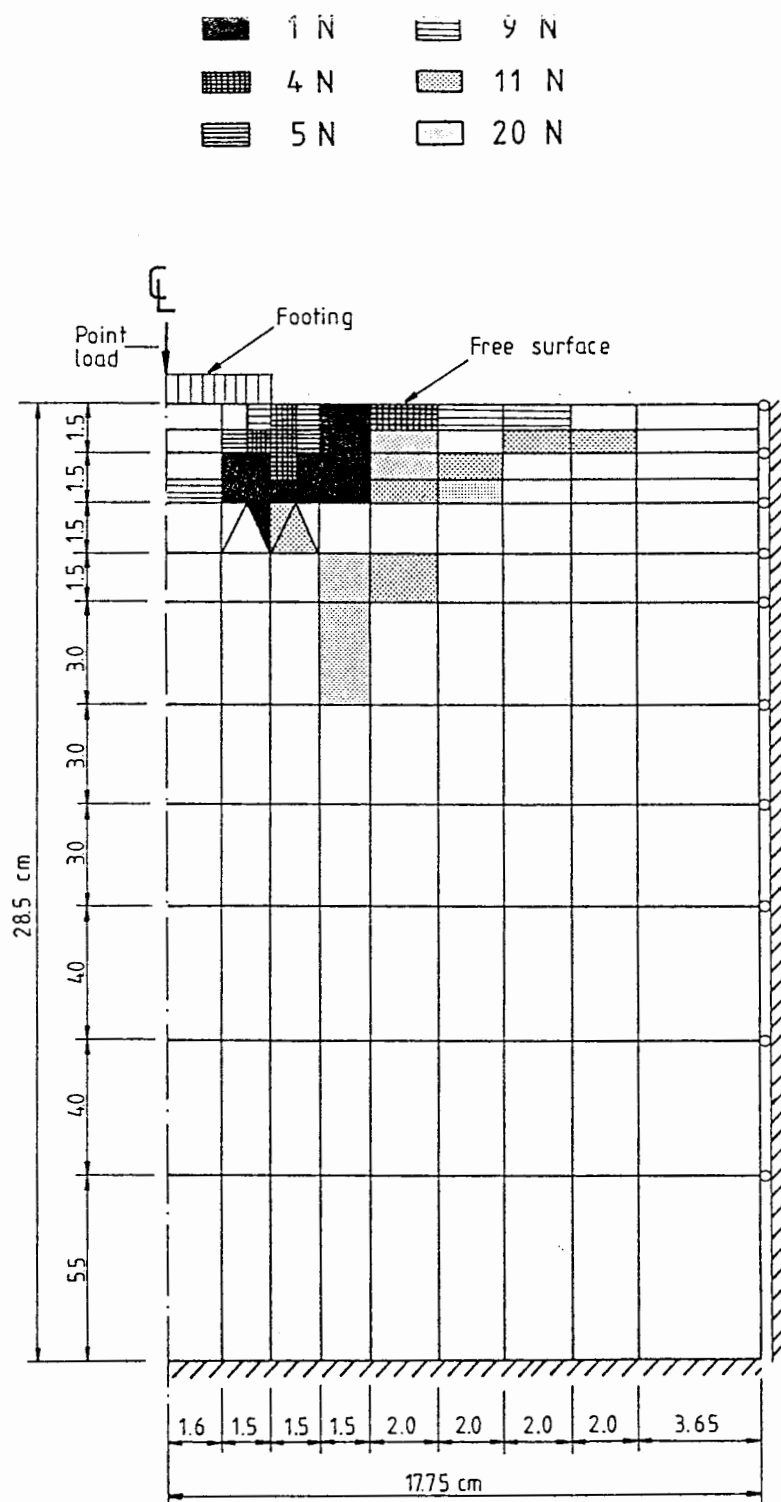


Figure 29. Failure Generation During AXISYM Analysis.

CHAPTER VI

MODEL FOUNDATION STUDY

In the previous chapter the response of a foundation was analytically investigated by means of the finite element code AXISYM. In order to further evaluate the established link between hyperbolic parameters and the pressuremeter test, the aforementioned footing was built, instrumented and subjected to a concentric point load similar to the analytical problem.

MODEL FOUNDATION AND LOAD APPLICATION

A consolidometer brass loading cap was employed as a model foundation measuring 1.2 cm in thickness and 6.2 cm in diameter. With a weight of 372.3 g and a Young's modulus of 110000 MPa this may be considered rigid relative to the soil. From its original design the model footing was furnished with a hollow sphere on top so that, by insertion of a metal ball weighing 66.6 g, a normal load application was forced. The bearing capacity for the model footing was determined after G.G. Meyerhof (1955) as being 67 N.

The sand was placed in a cylindrical container with a diameter of 35.5 cm and a height of 28.5 cm so that the depth of the container measured more than 4.5 times the

footing diameter. The placement procedure for the sand was similar to the one used for the pressuremeter tests, except that the sand was sieved into the container from a height of 15 cm. The application of high frequency (175 Hz) vibrations by means of a 3.5 cm diameter vibrating concrete poker, along the outer wall of the container yielded a relative density of $D_r = 70 \%$. The uniformity of the sand specimen was confirmed using cone penetration tests and only insignificant changes could be detected.

FOUNDATION TESTING PROCEDURE AND RESULTS

For this model foundation study the previously used triaxial test apparatus has been employed as a loading frame for the model foundation, allowing a smooth and gradual load application and settlement readings at the footing center.

The brass footing was placed on the levelled sand surface in the center of the container as shown. After the dial gauge was mounted and initialized, the load was gradually applied by the triaxial gear box up to a maximum force of 225 N (by far exceeding the calculated bearing capacity) at which a settlement of 2.5 cm was measured. Applied load measurements were taken every 0.127 mm of settlement at the footing center corresponding to 0.02 % of the footing diameter. Fig. 30 is a graphical display of the foundation response as measured in the loading frame.

Repeat tests showed almost identical results and the

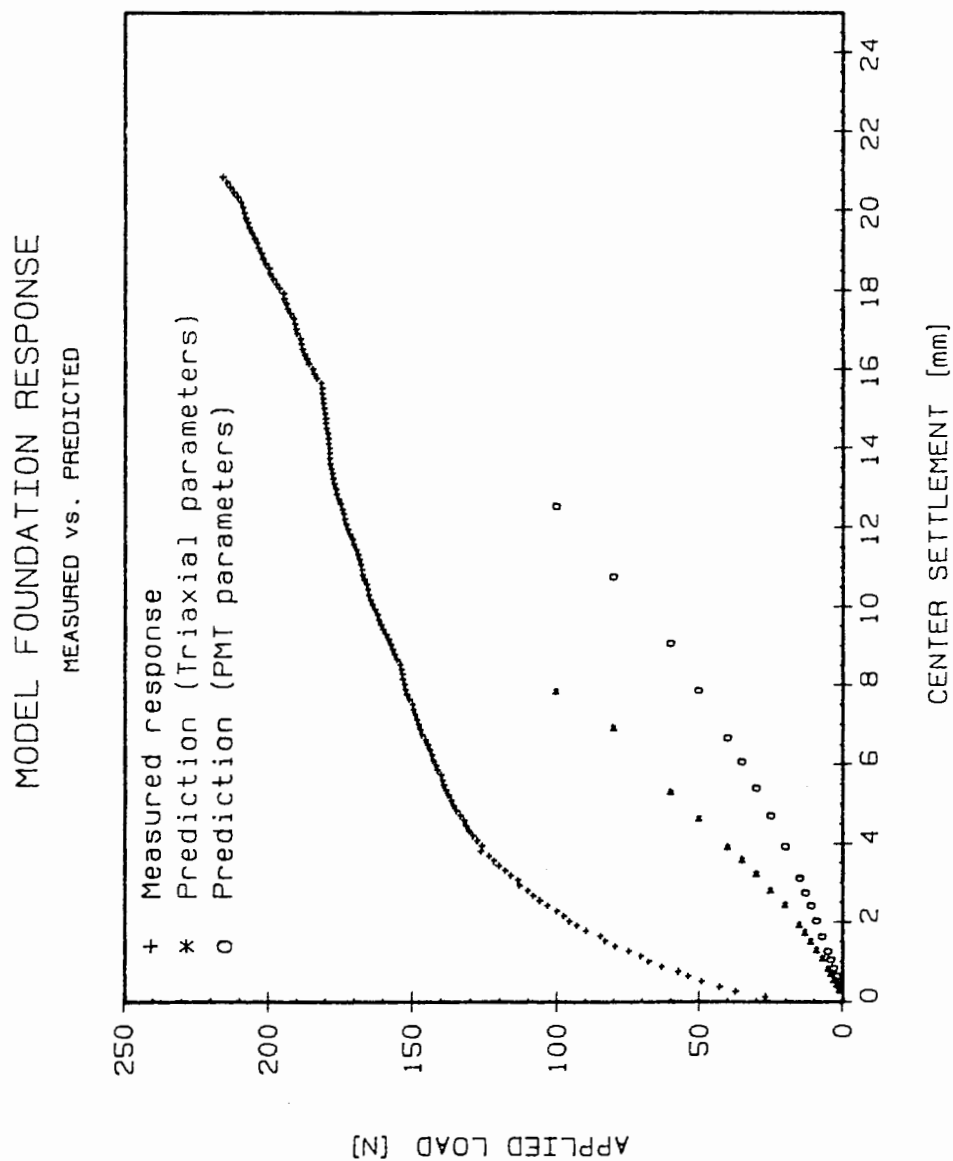


Figure 30. Load-Deflection Response
as Measured for the Model Foundation.

addition of dial gauges on the edge of the footing confirmed that no tilt took place upon load application.

Comparing the predicted (Fig. 28) to the measured settlements (Fig. 30) at the footing surface it is recognized, that only poor agreement is achieved, compared to the measured deflections. The deviation of predicted (using parameters based on pressuremeter tests) and measured deflections is explained by the very low modulus number used. Violation of the plane strain assumption during pressuremeter testing is a possible source of error. An additional factor of influence is suspected to be introduced by the placement procedure for the sand. Grains raining down in the vicinity of the probe are likely to contact the probe prior to final deposition leading to an area of looser material surrounding the probe.

A second execution of the problem using the parameters from triaxial tests resulted in much better agreement to the measured deflections as Fig. 30. shows.

CHAPTER VII

CASE HISTORY

A final evaluation of the proposed link between pressuremeter tests and the hyperbolic soil model is accomplished using results from pressuremeter tests performed under field conditions as presented in the following.

SAND 'H' DEBRIS BASIN

To evaluate the stability of an earth retaining structure a number of prebored (NX size TEXAM probe) and driven (slotted tube) pressuremeter tests were performed (T.D. Smith and C.E. Deal, 1988). The investigated embankment shows severe longitudinal cracking due to a moisture sensitive foundation. Built on fan debris flow deposits comprised of stratified gravels, sands, and silts, conventional soil investigation methods fail to provide economical soil information because of the coarse grained materials ($\gamma_{dry} = 19 \text{ kN/m}^3$) involved.

A summary of the results for the conducted pressuremeter tests is presented in Table VII.

TABLE VII
PMT RESULTS FOR DRY SOIL

Depth [m]	σ_z' [kPa]	G [kPa]	E_M [kPa]	σ_f [kPa]	P_I [kPa]	P_L [kPa]
1.83	34.8	8034	21370	1250	1750	2929
1.83	34.8	1992	5300	270	570	687
2.74	52.1	6015	16000	400	1160	1406
3.66	69.5	2519	6700	300	650	826
4.57	86.8	3019	8030	300	550	907
6.10	115.9	4154	11050	700	1120	1623
7.62	144.8	4530	12050	900	1450	1935
9.61	182.6	2481	6600	600	880	1214
11.00	209.0	4549	12100	800	1380	1855

Based on the above tabulated pressuremeter test results the hyperbolic parameters have been calculated using the proposed set of equations, assuming a cohesionless material. The computed parameters are presented in Table VIII and compared to the typical values recommended by M.G. Katona et al. (1981), where the correct order of magnitude is found.

TABLE VIII
HYPERBOLIC PARAMETERS - STANDARD vs. PMT

Parameter	CANDE recommendation	Pressuremeter test
K	200	90
n	0.4	0.6
ϕ	33.0	35.0
R_f	0.70	0.73
K_b	50	140
m	0.2	0.12

Finite element modelling using the above parameters within the finite element program FEADAM (J.M. Duncan, K.S. Wong and Y. Ozawa, 1980) resulted in similar distress features as those observed at the real embankment.

CHAPTER VIII

DISCUSSION OF THE RESULTS

An investigation has been carried out to explore the potential of the pressuremeter for the derivation of non-linear, stress-dependent parameters as input for finite element programs.

From this initial study it is clear that the calculation of parameters for soil models from pressuremeter tests might be, in general, the right step towards an approximation of the reliability of soil input to the high standards of finite element programs. This is also supported by findings of J.L. Kauschinger (1985) who successfully extracted parameters from pressuremeter data for J.H. Prévost's multi-yield surface model.

It is apparent that the accuracy of the proposed correlation between density and bulk modulus parameters is a function of the amount of incorporated data. Therefore an expansion of the data base would be desirable.

However, it must be pointed out that the foregoing study was limited to granular soils, where considerable volume changes occur due to compression and dilatancy. Those effects, among others, can not be modelled accurately using

the hyperbolic soil model. Therefore, if an attempt is made to model soils exhibiting such behavior, significant error can be introduced.

In addition, the function of the tangent modulus in the hyperbolic soil model is not continuous, as a brief inspection of Fig. 3 reveals. Even though this discontinuity may seem negligible it might result, incorporated into an incremental finite element calculation, in additional iterations, as H. Schad (1979) stated.

CONCLUSIONS AND RECOMMENDATIONS

During this investigation it became apparent that the construction material soil displays such a diversity of conditions that it does seem neither possible, nor meaningful, to develop a single soil model from which parameters are easily obtained and which yields correct descriptions of all possible stress states under every possible boundary condition. Nevertheless, a number of conclusions can be drawn from the foregoing:

1. Pressuremeter testing should be employed in the absence of triaxial data to calculate parameters describing the soil behavior according to the hyperbolic soil model, even though it seems more appropriate to use the pressuremeter data directly without the constraints of correlations to conventional soil investigation methods.

2. Nonlinear modeling is essential in capturing the real soil behavior and is best employed in conjunction with finite element programs.

3. Finite element solutions utilizing the hyperbolic approach might be very adequate for many "up-to-failure" problems in geotechnical engineering, even though shortcomings are obvious since important factors like stress history, time dependency and strain softening of the soil can not be accounted for.

4. A parametric study to investigate the sensitivity of the hyperbolic soil model, in its various stages of development, to deviations of the parameters from their determined values is recommended in order to evaluate the significance of errors introduced hereby.

5. The step increase of poisson's ratio at failure is not a realistic representation of the actual soil behavior. The bulk modulus formulation eliminates this problem by use of a hyperbolic function for the volume changes which have to be compressive, even though the test data may indicate dilation.

6. The development of a generalized constitutive law for soils represents a formidable task for future research. Volume change effects and failure mechanisms are undoubtedly of prime importance and inhibit many problems to be solved.

7. In the development of new models the derivation of the coefficients has to be realistically considered. Clearly, an integration of soil tests and model theory is absolutely necessary. It could be stated that any soil model is only as good as the soil test employed to find the parameters.

8. Laboratory pressuremeter testing turned out to be difficult to accomplish at small scale since considerable confining pressures were necessary to satisfy the plane strain condition. Moreover, adequate demonstration of the impact of increasing depth on the pressuremeter modulus and the limit pressure could not be made. Since chamber testing is an essential part of research in geotechnical engineering the availability of such a chamber is very much recommended.

LIST OF REFERENCES

- Baguelin, F., Jezequel, J.-F., and Shields, D.H., The Pressuremeter and Foundation Engineering, Trans-Tech Publications, Clausthal, West-Germany, 1978.
- Bishop, A.W., and Henkel, D.J., The Measurement of Soil Properties in the Triaxial Test, Second Edition, Edward Arnold Publishers, London, United Kingdom, 1962.
- Bowles, J.E., Foundation Analysis and Design, Third Edition, McGraw-Hill Book Company, New York, United States, 1982.
- Briaud, J.-L., Lytton, R.L., and Hung, J.-T., "Obtaining Moduli from Cyclic Pressuremeter Tests," Journal of the Soil Mechanics and Foundation Division, ASCE, Vol. 109, No. 5, May, 1983, pp. 657-665.
- Briaud, J.-L., and Shields, D.H., "Pressuremeter Tests At Very Shallow Depth," Journal of the Soil Mechanics and Foundation Division, ASCE, Vol. 107, No. GT8, August, 1981, pp. 1023-1040.
- Briaud, J.-L., Tucker, L.M. and Makarim, C.A., "Pressuremeter Standard and Pressuremeter Parameters," The Pressuremeter and Its Marine Applications: Second International Symposium, ASTM STP 950, Texas, 1986.
- Centre d'Etudes Ménard, "Règles d'Utilisation des Techniques Pressiométriques et d'Exploitation des Résultats Obtenus pour le Calcul des Fondations", Publication D/60/75, France, 1975.
- Cornforth, D.H., "Prediction of Drained Strength of Sands from Relative Density Measurements," Special Technical Publication 523, ASTM Evaluation of Relative Density and its role in Geotechnical Projects Involving Cohesionless Soils, 1973, pp. 281-303.
- Cox, H., "The Deflection of Imperfectly Elastic Beams and the Hyperbolic Law of Elasticity," Transactions of the Cambridge Philosophical Society, Part 2, 9, 1850, pp. 177-190.
- Desai, C.S., and Christian, T., Numerical Methods in Geotechnical Engineering, McGraw-Hill Book Company, USA, 1977.

- Dorairaja, R. , "Finite Element Analysis of the Behavior of Nonlinear Soil Continua Including Dilatancy," A Dissertation submitted to the Graduate Faculty of Texas Tech University, in partial fulfillment of the requirements for the Degree of Doctor of Philosophy, 1975.
- Duncan, J.M., and Chang, C.Y., "Nonlinear Analysis of Stress and Strain in Soils," Journal of the Soil Mechanics and Foundation Division, ASCE, Vol. 96, No. SM5, September, 1970, pp. 1629-1653.
- Duncan, J.M., Byrne, P., Wong, K.S., and Mabry, P., "Strength, Stress-Strain and Bulk Modulus Parameters for Finite Element Analyses of Stresses and Movements in Soil Masses," Report No. UCB/GT/80-01, University of California, Berkeley, California, August 1980.
- Duncan, J.M., Wong, K.S., and Ozawa, Y., "FEADAM: A Computer Program for Finite Element Analysis of Dams," Report No. UCB/GT/80-02, University of California, Berkeley, California, December 1980.
- Felio, G.J., and Briaud, J.-L., "Conventional Parameters from Pressuremeter Test Data: Review of Existing Methods," The Pressuremeter and Its Marine Applications, Second International Symposium, ASTM STP 950, Texas, 1986.
- Gallagher, R.H., Finite Element Analysis: Fundamentals, Prentice Hall, Englewood Cliffs, New Jersey, 1975.
- Hartman, J.P., "Finite Element Parametric Study of Vertical Strain Influence Factors and the Pressuremeter Test to Estimate the Settlement of Footings in Sand," Thesis presented to the University of Florida, in partial fulfillment of the requirements for the Degree of Doctor of Philosophy, 1974.
- Herrmann, L.R., "Elasticity Equations for Incompressible and Nearly Incompressible Materials by a Variational Theorem," AIAA Journal, Vol. 3, No. 10, pp. 1896-1900, October, 1965.
- Holloway, D.M., "User's Manual for Axisym: A Finite Element Program for Axisymmetric or Plane Strain Simulation of Soil-Structure Interaction," Contract Report S-76-13 U.S. Army Eng. Waterw. Expt. Stn., Vicksburg, Miss. 1976.

- Janbu, N., "Soil Compressibility as Determined by Oedometer and Triaxial Tests," European Conference on Soil Mechanics and Foundation Engineering, Wiesbaden, Germany, Vol.1, pp. 19-25, 1963.
- Johnson, L.D., "Correlation of Soil Parameters from In Situ and Laboratory Tests for Building 333," Proceedings of the ASCE Specialty Conference on Use of In Situ Tests in Geotechnical Engineering, Virginia Polytechnic Institute and State University, June, 1986.
- Katona, M.G., Vittes, P.D., Lee, C.H. and Ho, H.T., "CANDE-1980: Box Culverts and Soil Models," Report No. FHWA/RD-80/172, Notre Dame, Indiana, May, 1981.
- Kauschinger, J.L., "Interim Report: Extracting Multi-Yield Surface Model Parameters from Pressuremeter Data," A Report on Research sponsored by the Engineering Foundation of ASCE under Research Contract No. RI-A-84-2, Medford, Massachusetts, July 1985.
- Kögler, F., "Baugrundprüfung im Bohrloch," Der Bauingenieur, Heft 19-20, pp. 266-270, Berlin, Germany, 1933.
- Kolbuszewski, J.J., and Jones, R.H., "The Preparation of Sand Samples for Laboratory Testing," Proceedings of the Midland Soil Mechanics and Foundation Engineering Society, Vol. 4., Birmingham, England, 1961.
- Kolbuszewski, J.J., "General Investigation of the Fundamental Factors Controlling Loose Packing of Sands," Proceedings of the Second International Conference on Soil Mechanics, Vol.7, pp. 47-49, Rotherdam, Netherlands, 1948.
- Kolbuszewski, J.J., "An Experimental Study of the Maximum and Minimum Porosities of Sands," Proceedings of the Second International Conference on Soil Mechanics, Vol.1, pp. 158-165, Rotherdam, Netherlands, 1948.
- Kondner, R.L., "Hyperbolic Stress-Strain Response: Cohesive Soils," Journal of the Soil Mechanics and Foundation Division, ASCE, Vol. 89, No. SM1, February, 1963, pp. 115-143.
- Kondner, R.L., Zelasko, S.S., "A Hyperbolic Stress-Strain Formulation of Sands," Proceedings of the 2nd PanAmerican Conference on Soil Mechanics and Foundation Engineering, Vol. 1, Brazil, 1963, pp. 289-324.

- Kulhawy, F.H., Duncan, J.M. and Seed, H.B., "Finite Element Analyses of Stresses and Movements in Embankments During Construction," U.S. Army Eng. Waterw. Expt. Stn. Contract Report 569-8, Vicksburg, Miss., 1969.
- Lade, P.V., "Cubical Triaxial Apparatus for Soil Testing," Geotechnical Testing Journal, No. 1, 1979, pp.93-101.
- Livneh, M., Gilbert, M., and Uzan, J., "Determination of the Elastic Modulus of Soil by the Pressuremeter Test-Theoretical Background," Journal of Materials, Vol. 6, No. 2, June 1971.
- MacNeal, R.H., and Harder, R.H., "A Proposed Set of Problems to Test the Finite Element Accuracy", 25th SDM Finite Element Validation Forum, Palm Springs, 1984.
- McCormack, T.C., "A Finite Difference Soil-Structure Interaction Study of a Section of the Bonneville Navigation Lock Buttress Diaphragm Wall Utilizing Pressuremeter Test Results," M. Sc. Thesis, submitted in partial fulfillment of the requirements for the degree of Master of Science, Portland State University, 1987.
- Ménard, L., "An Apparatus for Measuring the strength of Soils in Place," M. Sc. Thesis, University of Illinois, 1957.
- Ménard, L., "Influence de l'amplitude et de l'histoire d'un champ de contraintes sur le tassement d'un sol de fondation," Proceedings of the Fifth International Conference on Soil Mechanics and Foundation Engineering, Paris, 1961, Vol. 1, pp. 249-253.
- Meyerhof, G.G., "Influence of Roughness Base and Groundwater Conditions on the Ultimate Bearing Capacity of Foundations," Geotechnique, Vol. V, 1955, pp. 227-242.
- Mulilis, J.P., Seed, H.B., Chan, C.K., Mitchell, J.K., and Arulanandan, K., "Effects of Sample Preparation on Sand Liquefaction," Journal of the Soil Mechanics and Foundation Division, ASCE, Vol. 103, No. GT2, February, 1977, pp. 91-108.
- Pierce, J.A., "A New True Triaxial Apparatus," Stress-Strain Behaviour of Soils. Roscoe Memorial Symposium, 1971, pp. 330 - 339.

- Poulos, H.G., and Davis, E.H., Elastic Solutions for Soil and Rock Mechanics, John Wiley and Sons, New York, 1974.
- Prévost, J.-H., "Anisotropic Undrained Stress-Strain Behaviour of Clays," Journal of the Soil Mechanics and Foundation Division, ASCE, Vol. 104, No. GT8, August, 1978, pp. 1075-1090.
- Schad, H., "Nichtlineare Stoffgleichungen für Böden und ihre Verwendung bei der numerischen Analyse von Grundbauaufgaben," Mitteilung Nr. 10 des Baugrundinstituts Stuttgart, West Germany, 1979.
- Smith, T.D., "Pressuremeter Design Method for Single Piles Subjected to Static Lateral Load," Dissertation submitted to the Graduate College of Texas A&M University, in partial fulfillment of the requirements for the Degree of Doctor of Philosophy, 1983.
- Smith, T.D., and Deal, C.E., "Cracking Studies at Sand H Debris Basin by the Finite Element Method," to be published in Proceedings of the Second International Conference on Case Histories in Geotechnical Engineering, St. Louis, Missouri, June, 1988.
- Spangler, M.G., Handy, R.L., Soil Engineering, Fourth Edition, Harper & Row Publishers, New York, 1982.
- Tranter, C.J., "On the Elastic Distortion of a Cylindrical Hole by a Localized Hydrostatic Pressure," Quarterly of Applied Mathematics, Vol. 4, No. 3, 1946.
- Turner, M.J., Clough, R.W., Martin, H.C., and Topp, L.J., "Stiffness and Deflection Analysis of Complex Structures," Journal of the Aeronautical Sciences, Vol. 23, No. 9, September 1956.
- Wroth, C.P., and Windle, D., "Analysis of the Pressuremeter Test allowing for Volume Change," Geotechnique, Vol. XXV, Number 3, September, 1975, pp. 598-604.
- Wroth, C.P., "British Experience with the Selfboring Pressuremeter," Symposium on the Pressuremeter and its Marine Applications, IFP, Paris, April 1982.

LIST OF NOTATIONS

a	Initial tangent modulus constant.
b	Ultimate stress difference constant.
B	Bulk modulus.
c	Cohesion.
D_r	Relative density.
E	Young's modulus, modulus of elasticity.
E_i	Initial tangent modulus.
E_m	Pressuremeter modulus of micro-deformation.
E_M	Menard modulus based on $\nu = 0.33$.
E_{PM}	Modified pressuremeter modulus.
E_s	Soil modulus.
E_t	Tangent modulus.
E_{ur}	Unload-reload modulus.
G	Shear modulus.
K	Modulus number.
K_0	At rest earth pressure coefficient.
K_a	Active earth pressure coefficient.
K_b	Bulk modulus number.
K_{PM}	Modulus number from pressuremeter test.
K_{pur}	Unload-reload modulus number from pressuremeter test.
K_{ur}	Unload-reload modulus number.
L/D	Length to diameter ratio.
m	Bulk modulus exponent.

n	Modulus exponent.
P_a	Atmospheric pressure.
P_L	Theoretical limit pressure.
P_I	Practical limit pressure.
P_I^*	Net limit pressure.
P_0	Total initial horizontal stress.
P_{0M}	Pressure at the start of the straight line portion of the pressuremeter test curve.
R_f	Failure ratio.
R_{pf}	Failure ratio based on pressuremeter test.
r	Radial distance.
r_0	Initial cavity radius.
s	Modulus exponent from pressuremeter test.
S	Stress level.
α_F	<i>Almansi</i> strain at failure.
δ or Δ	Change of
ϵ_0	Cavity strain.
ϵ_a	Axial strain.
ϵ_r	Radial strain.
ϵ_{vol}	Volumetric strain.
ϵ_z	Vertical strain.
ϕ	Angle of internal friction.
ϕ_{cv}	Angle of internal friction at constant volume.
ϕ_{dc}	Density component for angle of internal friction.

$\Delta\phi$	Change in angle of internal friction.
γ_{dry}	Dry unit weight.
γ_{yz}	Shear strain.
ν	Poisson's ratio.
ν_f	Poisson's ratio at failure.
σ_1	Major principal stress.
σ_2	Intermediate principal stress.
σ_3	Minor principal stress.
σ_r	Radial stress at failure.
σ_h'	Effective horizontal stress.
σ_n	Normal stress.
σ_r	Radial stress.
σ_z'	Effective vertical stress.
σ_θ	Circumferential stress.
σ_{oct}	Octahedral stress.
τ	Shear stress.
τ_{max}	Maximum shear stress.
τ_{yz}	Shear stress in axisymmetric coordinates.
θ_f	Angle of failure plane.

APPENDIX

Site: <u>PSU</u>	Soil: <u>Willamette RS, 60%</u>	Test No.: <u>Drum I</u>	Depth: <u>0.57 m</u>	Quality: ¹⁾ <u>*</u>
------------------	---------------------------------	-------------------------	----------------------	---------------------------------

Measured information:

$$p_0 = \underline{7 \text{ KPa}} \quad \sigma_f = \underline{16 \text{ KPa}} \quad p_l = \underline{33 \text{ KPa}}$$

Calculated from curve:

$$G = \underline{325 \text{ KPa}} \quad E = \underline{865 \text{ KPa}} \quad (\nu = 0.33)$$

Remarks: p_t by manual extrapolation, unusual shape of curve for sand, difficult interpretation, ϕ' based on Eq. 3-26.

Theoretical values:

$$p_0 = \underline{2.84 \text{ KPa}} \quad \sigma_f = \underline{4.74 \text{ KPa}} \quad p_l = \underline{32.5 \text{ KPa}} \quad p_L = \underline{35.7 \text{ KPa}}$$

Remarks: p_0 based on $K_0 = 0.4$, $\sigma'_z = 8.61 \text{ KPa}$, $\phi' = 41.9^\circ$

Hyperbolic Parameters:

$$R_{pf} = \frac{p_l}{p_L} = \frac{\text{THEORY, MEASURED}}{0.74/0.75} \quad m = \underline{0.09} \quad K_b = \underline{556}$$

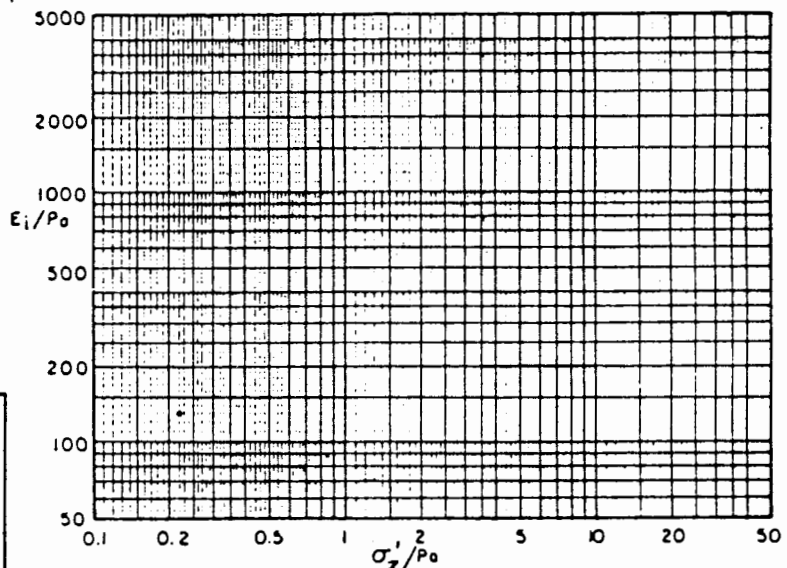
$$K_{PM} = \underline{84}$$

$$s = \underline{0.51}$$

K_{PM} & s see next page.

D_c influenced?

- 1) * Poor quality, only limited value.
 ** Good quality, lacking in some areas.
 *** Excellent quality.



Site: <u>PSU</u>	Soil: <u>Willamette RS, 68%</u>	Test No.: <u>Drum II</u>	Depth: <u>1.47 m</u>	Quality: ¹⁾ <u>**</u>
------------------	---------------------------------	--------------------------	----------------------	-------------------------------------

Measured information:

$$p_0 = \underline{14 \text{ kPa}} \quad \sigma_f = \underline{26.5 \text{ kPa}} \quad p_l = \underline{49 \text{ kPa}}$$

Calculated from curve:

$$G = \underline{495 \text{ kPa}} \quad E = \underline{1317 \text{ kPa}} \quad (\nu = 0.33)$$

Remarks: see previous page

Theoretical values:

$$p_0 = \underline{8.88 \text{ kPa}} \quad \sigma_f = \underline{14.81 \text{ kPa}} \quad p_l = \underline{74.2 \text{ kPa}} \quad p_L = \underline{100.4 \text{ kPa}}$$

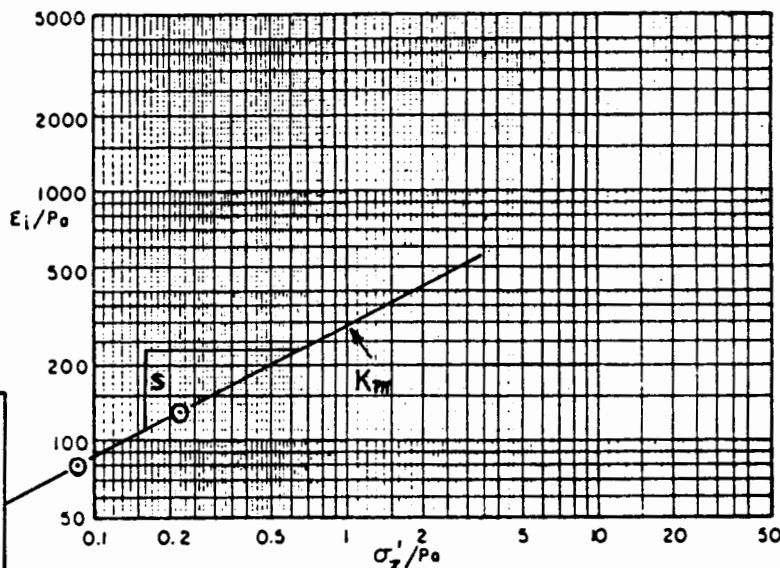
Remarks: p_0 based on $K_0 = 0.4$, $\sigma'_z = 22.2 \text{ kPa}$

Hyperbolic Parameters:

$$R_{pf} = \frac{p_l}{p_L} = \frac{\text{Theory}}{\text{MEASURED}} = \underline{0.74/0.49} \quad m = \underline{0.09} \quad K_b = \underline{556}$$

$$K_{PM} = \underline{84}$$

$$s = \underline{0.51}$$



- 1) * Poor quality,
only limited value.
** Good quality,
lacking in some areas.
*** Excellent quality.

Site: _____	Soil: _____	Test No.: _____	Depth: _____	Quality: ¹⁾ _____
-------------	-------------	-----------------	--------------	------------------------------

Measured information:

$$p_o = \text{_____} \quad \sigma_f = \text{_____} \quad p_l = \text{_____}$$

Calculated from curve:

$$G = \text{_____} \quad E = \text{_____}$$

Remarks: _____Theoretical values:

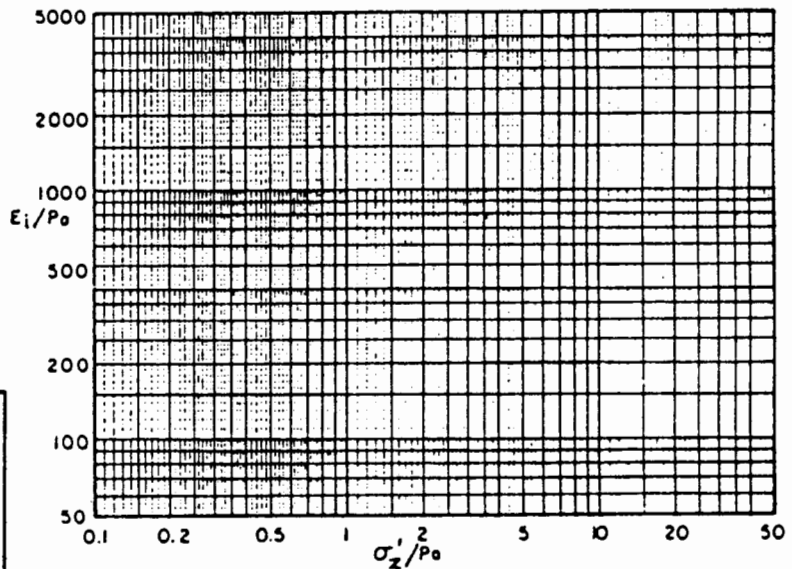
$$p_o = \text{_____} \quad \sigma_f = \text{_____} \quad p_l = \text{_____} \quad p_L = \text{_____}$$

Remarks: _____Hyperbolic Parameters:

$$R_{pf} = \frac{p_l}{p_L} = \text{_____} \quad m = \text{_____} \quad K_D = \text{_____}$$

$$K_{PM} = \text{_____}$$

$$S = \text{_____}$$



- 1) * Poor quality,
only limited value.
- ** Good quality,
lacking in some areas.
- *** Excellent quality.